Check for updates

JOURNAL OF QUATERNARY SCIENCE (2021) **36**(5) 780–804 ISSN 0267-8179. DOI: 10.1002/jqs.3313

JQS Journal of Quaternary Science QRA Quaternary Research Association

Maximum extent and readvance dynamics of the Irish Sea Ice Stream and Irish Sea Glacier since the Last Glacial Maximum

J. D. SCOURSE,[1]* R. C. CHIVERRELL,[2] R. K. SMEDLEY,[2] D. SMALL,[3] M. J. BURKE,[2] M. SAHER,[4] K. J. J. VAN LANDEGHEM,[4] G. A. T. DULLER,[5] C. Ó COFAIGH,[3] M. D. BATEMAN,[6] S. BENETTI,[7] S. BRADLEY,[6] L. CALLARD,[8] D. J. A. EVANS,[3,7] D. FABEL,[9] G. T. H. JENKINS,[5] S. MCCARRON,[10] A. MEDIALDEA,[11] S. MORETON,[12] X. OU,[5,15] D. PRAEG,[13,14] D. H. ROBERTS,[3] H. M. ROBERTS[5] and C. D. CLARK[6]

[1]Centre for Geography and Environmental Science, University of Exeter, Penryn, UK
[2]School of Environmental Sciences, University of Liverpool, Liverpool, UK
[3]Department of Geography, Durham University, Durham, UK
[4]School of Ocean Sciences, Bangor University, Menai Bridge, UK
[5]Department of Geography and Earth Sciences, Aberystwyth University, Aberystwyth, UK
[6]Department of Geography, University of Sheffield, Sheffield, UK
[7]School of Geography and Environmental Sciences, Ulster University, Coleraine, UK
[8]School of Geography, Politics and Sociology, University of Newcastle, Newcastle, UK
[9]Scottish Universities Environmental Research Centre, East Kilbride, UK
[10]Department of Geography, Maynooth University, Maynooth, Ireland
[11]CENIEH (Centro Nacional de Investigación sobre la Evolución Humana), Burgos, Spain
[12]NERC Radiocarbon Laboratory, East Kilbride, UK
[13]OGS (Istituto Nazionale di Oceanografia e di Geofisica Sperimentale), Borgo Grotta Gigante, Trieste, Italy
[14]Laboratório de Geologia Marinha, Universidade Federal Fluminense, Brazil
[15]School of Geography and Tourism, Jiaying University, Meizhou, China

Received 2 September 2020; Revised 3 March 2021; Accepted 18 March 2021

ABSTRACT: The BRITICE-CHRONO Project has generated a suite of recently published radiocarbon ages from deglacial sequences offshore in the Celtic and Irish seas and terrestrial cosmogenic nuclide and optically stimulated luminescence ages from adjacent onshore sites. All published data are integrated here with new geochronological data from Wales in a revised Bayesian analysis that enables reconstruction of ice retreat dynamics across the basin. Patterns and changes in the pace of deglaciation are conditioned more by topographic constraints and internal ice dynamics than by external controls. The data indicate a major but rapid and very short-lived extensive thin ice advance of the Irish Sea Ice Stream (ISIS) more than 300 km south of St George's Channel to a marine calving margin at the shelf break at 25.5 ka; this may have been preceded by extensive ice accumulation plugging the constriction of St George's Channel. The release event between 25 and 26 ka is interpreted to have stimulated fast ice streaming and diverted ice to the west in the northern Irish Sea into the main axis of the marine ISIS away from terrestrial ice terminating in the English Midlands, a process initiating ice stagnation and the formation of an extensive dead ice landscape in the Midlands. © 2021 The Authors *Journal of Quaternary Science* Published by John Wiley & Sons, Ltd.

KEYWORDS: deglaciation; geochronology; geomorphology; ice stream; marine geology

Introduction

The Irish Sea Ice Stream (ISIS) was the largest ice stream draining the former British–Irish Ice Sheet (BIIS; Fig. 1A). Extending for some 750 km from feeder catchment uplands in southwestern Scotland, eastern Ireland, the English Lake District, Snowdonia and west Wales, it flowed southwards through the Irish Sea Basin (ISB). During its maximum extent, it penetrated and crossed the Celtic Sea to a marine terminus south of St George's Channel (Fig. 1A). ISIS was, however, unique in the BIIS context in that it was a compound ice stream with a secondary terrestrial non-streaming terminal zone in the English Midlands, here defined as the Irish Sea Glacier (ISG; Fig. 1A; Thomas, 1985, 1989, 2005; Chiverrell *et al.*, 2020) with a bifurcation zone north of the current North Wales coast; please note that the term Irish Sea Glacier has previously been used to denote ice more generally within the ISB but is used in this more restricted sense here (cf. Lewis and Richards, 2005). Unlike some of the other ice streams draining the former BIIS, the significance of the ISIS has been recognized for over 100 years (Wright, 1914) based on erratic trains, notably of Ailsa Craig microriebeckite and Shap granite (Fig. 1A), till matrix lithologies and landform distribution; 'Irish Sea Till', though spatially variable, has been a mappable lithostratigraphic unit along the margins of the Irish and Celtic seas readily distinguishable from more local tills of inland ice source on the basis of colour (dark blue–grey in the south, red in the north), lithology, high matrix to clast ratio and, above all, the incorporation of marine carbonate macro- and microfauna (e.g. Austin and McCarroll, 1992) giving rise to the designation 'shelly till'. In parallel with the description and process understanding of ice streams within contemporary ice sheets (e.g.

*Correspondence: J. Scourse, as above.
E-mail: j.scourse@exeter.ac.uk

© 2021 The Authors *Journal of Quaternary Science* Published by John Wiley & Sons, Ltd.
This is an open access article under the terms of the Creative Commons Attribution License, which permits use, distribution and reproduction in any medium, provided the original work is properly cited.

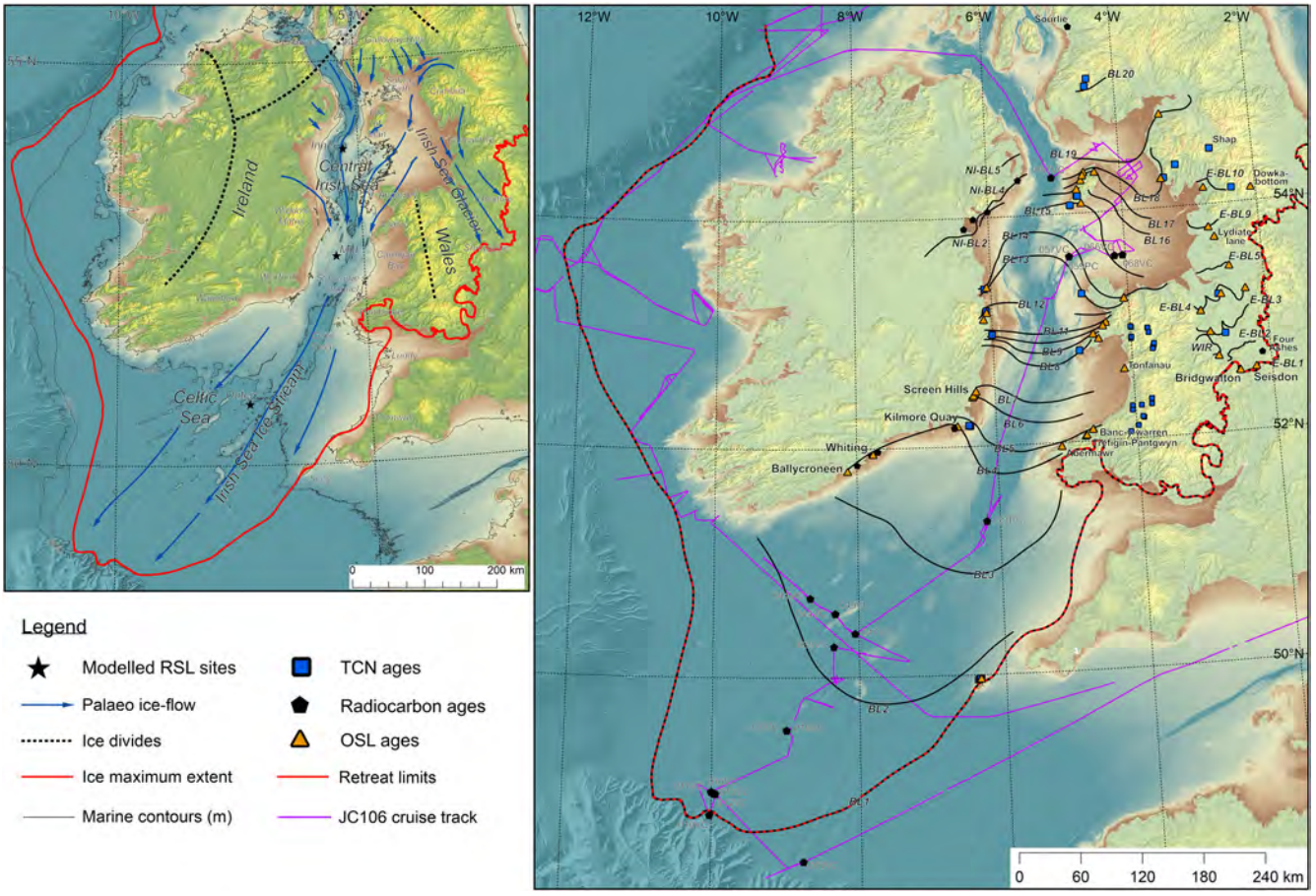

Figure 1. Location maps plotted over the CGIAR-CSI SRTM (Version 4) 30-m-resolution topography (http://srtm.csi.cgiar.org/srtmdata/) and EMODnet bathymetric data (https://www.emodnet-bathymetry.eu/). (A) The Irish Sea Ice Stream (ISIS) and Irish Sea Glacier (ISG), place names, ice maximum extent, ice flow lines, ice divides (as maximum glaciation) based on Clark *et al.* (2012) apart from the divide in the Galloway Hills based on Finlayson *et al.* (2010), major bathymetric contours, and the inner, mid- and outer locations for modelled relative sea level (RSL) water depths from a glacio-isostatic adjustment model (Bradley *et al.*, 2011). (B) The retreat patterns of the ISIS and ISG (Fig. 8) identifying the Boundary limits (BL), typically well-defined ice margin limit positions that punctuated the Prior models used in the Bayesian modelling (Fig. 6). ISIS limits are BL1 to BL22, ISG limits in the English Midlands E-BL1 to E-BL10 and in northeast Ireland NI-BL2, 4 and 5. Sample location names and the sampling track of the RRS *James Cook* cruise (JC106) are also shown. [Color figure can be viewed at wileyonlinelibrary.com].

Alley *et al.*, 1986), the identification of marginal fast flow sectors in the form of drumlin fields (Clark *et al.*, 2012) and clear evidence of ice streaming on the floor of the Irish Sea (Van Landeghem *et al.*, 2009; Van Landeghem and Chiverrell, 2020) confirmed the recognition that the Irish Sea system was indeed a former ice stream (Roberts *et al.*, 2007).

Despite earlier interpretations that the Irish Sea Till might pre-date the last glacial stage, based purely on lithostratigraphy (Mitchell, 1972; Bowen, 1973), the gradual accumulation of geochronological evidence over the past 30 years has forced the realization that the Irish Sea Till is overwhelmingly of last glacial stage age. Indeed, the richness of this legacy of geochronological data constraining the advance, maximum extent, retreat and readvance phases of the BIIS enabled the first application of Bayesian analysis to any retreating ice stream (Chiverrell *et al.*, 2013). These geochronological data included optically stimulated luminescence (OSL) ages on proximal glacifluvial sequences, terrestrial cosmogenic nuclide (TCN) ages on glacially transported boulders and glacially scoured bedrock surfaces, and radiocarbon ages (^{14}C) on materials from below, within and above glacigenic units. This analysis enabled the identification of outliers and reduction in the uncertainty of individual determinations. The reconstruction emerging from this analysis was of advance of the ice stream between 30 and 24.3 ka to a maximum limit in the central Celtic Sea (Scourse *et al.*, 1990) to the southwest of the Isles of Scilly (Scourse, 1991) between 25.3 and 24.5 ka, before rapid but stepped northwards retreat with readvance phases out of the Celtic Sea into the northern Irish Sea. The timing of the maximum extent of this advance was corroborated by the independent dating of ice-rafted detritus (IRD) sourced from the Celtic Sea in a deep-sea core from the Goban Spur adjacent to the ISIS terminus in the Celtic Sea to between 24 and 25 ka (Scourse *et al.*, 2009; Haapaniemi *et al.*, 2010).

The demonstration that Bayesian analysis could be successfully applied to geochronological series constraining ice stream dynamics, and the quantification of IRD flux from the BIIS in the adjacent deep-sea sequences, were key motivations behind the establishment in 2012 of the BRITICE-CHRONO Consortium Project (Small *et al.*, 2017). Even though, at the onset of the project, the ISIS was the best constrained ice stream draining the former BIIS, there were significant uncertainties concerning the dynamics of the ice stream. These included defining the maximum extent of the ISIS in the Celtic Sea sector, establishing the retreat dynamics of the ice stream as it backstepped towards St George's Channel, constructing a chronology for the multiple readvance sequences identified in southeast Ireland (Screen Hills; Thomas & Summers, 1983, 1984) and the Llŷn Peninsula in north Wales (Thomas and Chiverrell, 2007) and across the Isle of Man (Thomas *et al.*, 2004), establishing a retreat chronology for the dynamics of the English Midlands lobe (ISG; Thomas, 1989; Chiverrell *et al.*, 2016) and defining the nature and timing of the bifurcation between the ISIS and English Midlands ice. It was not known whether the retreating terminus within the Celtic and Irish

© 2021 The Authors *Journal of Quaternary Science* Published by John Wiley & Sons, Ltd.

10991417, 2021, 5, Downloaded from https://onlinelibrary.wiley.com/doi/10.1002/jqs.3313 by Ogs Trieste Istituto Nazionale, Wiley Online Library on [24/11/2023]. See the Terms and Conditions (https://onlinelibrary.wiley.com/terms-and-conditions) on Wiley Online Library for rules of use; OA articles are governed by the applicable Creative Commons License

seas was everywhere marine, or whether it incorporated a component of terrestrial retreat on an emergent seabed (cf. Furze *et al.*, 2014), how the retreat sequence related to IRD flux on the adjacent margin, or how the changes in the rate of retreat related to the primary external forcings and controls such as atmospheric and marine climate, relative sea level, palaeotidal amplitudes, bed slope and topographic constrictions. To address these questions, constraining the retreat dynamics of the BIIS in the Irish Sea sector was defined as a core component of BRITICE-CHRONO, and two of the project transects, Transect 3 (T3; English Midlands lobe, ISG) and Transect 4 (T4; Celtic and Irish sea axis, ISIS) were established for detailed investigation (Fig. 1). Both transects involved the application of OSL and TCN techniques to terrestrial sequences, in marginal settings in the Isles of Scilly, east Ireland, west and north Wales (T4), and in the English Midlands lowlands, northwest England, southwest Scotland and the Isle of Man (T3). Sediment core material yielding samples for ^{14}C dating was acquired during investigation of the marine sequence for both transects during research cruise JC106 of the RRS *James Cook* during the summer of 2014 (Fig. 1B).

A series of sub-transect papers have been published reporting the detail of the new geochronological data and their stratigraphic context. These include terrestrial data from the Isles of Scilly (Smedley *et al.*, 2017a), southeast and east Ireland (Small *et al.*, 2018), the Llŷn Peninsula (Smedley *et al.*, 2017b), English Midlands (Chiverrell *et al.*, 2020), and offshore for the Celtic Sea (Lockhart *et al.*, 2018; Scourse *et al.*, 2019) and northern Irish Sea (Chiverrell *et al.*, 2018). The purpose of this paper is to provide a synthesis of the legacy and new BRITICE-CHRONO data for T3 and T4 presented in these sub-transect contributions, and to present a revised Bayesian analysis of these data. We present new geochronological data for three sites in west Wales, Abermawr, Banc-y-Warren and Tonfanau (Fig. 1B), and integrate these into this synthesis, which includes further independent data from southwest Wales published recently (Pantgwyn-Trefigin; Fig. 1B; Glasser *et al.*, 2018). The patterns, timing and rates of retreat of both the ISIS (T4) and the ISG (T3) are then compared with independent data on potential drivers of retreat to highlight the major forcings responsible for deglaciation. The contrast between the largely marine ISIS and largely terrestrial ISG sectors (Fig. 1) is particularly valuable in this context as a natural experiment because marine controls early in deglaciation (relative sea-level change, palaeotidal amplitude change, ocean heat supply) only apply for the ISIS.

Review of published data on ISIS and ISG maximum extent and deglacial chronologies

Isles of Scilly

The interpretation that the well-defined ice limit across the northern Isles of Scilly (Scourse, 1991; Hiemstra *et al.*, 2006) dated to the Late Devensian, and not an earlier glacial stage (cf. Mitchell and Orme, 1967; Bowen, 1973), was first proposed by Scourse (1991). The evidence for this was on the basis of conventional ^{14}C dating of organic deposits lying stratigraphically beneath the Scilly Till (Scourse, 1991) and some experimental thermoluminescence (TL; Wintle, 1981) and OSL ages (Smith *et al.*, 1990) on loessic material associated genetically with the Scilly Till. These data were later supplemented by OSL data from glacifluvial sands from north Tresco (Battery site; Scourse and Rhodes, 2006) and TCN ages on the Shipman Head Boulder Moraine and other bedrock surfaces by McCarroll *et al.* (2010); these data were also consistent with a glacial event during Marine Isotope Stage 2. None of these determinations were considered sufficiently robust to be included in the legacy dataset screened within BRITICE-CHRONO (Small *et al.*, 2017) so a further dating campaign was undertaken (Smedley *et al.*, 2017a). A series of OSL ages on glacifluvial outwash sand lenses at the Battery site (Tresco) indicated emplacement at 25.5 ± 1.5 ka and, together with TCN ages on boulders overlying till on Scilly Rock of 25.9 ± 1.6 ka, confirmed that ISIS impinged on the northern Isles of Scilly, but did not override the archipelago, at ~26 ka (Smedley *et al.*, 2017a). Scilly therefore constitutes a tightly dated ice-marginal position for the maximum extent of the eastern flank of ISIS within the Celtic Sea (Fig. 1).

Celtic Sea

Undated sporadic patches of till and glacimarine sediments found by the British Geological Survey to the west and southwest of Scilly in the Celtic Sea, constituting the Melville Till and Melville laminated Clay, respectively (Pantin and Evans, 1984; Scourse *et al.*, 1990) have long been considered a correlative of the Scilly Till (Scourse, 1991; Scourse and Furze, 2001). These remained undated until new cores of glacimarine sediment were recovered from close to the shelf break, one containing an Arctic mollusc yielding a ^{14}C age of $24\,265 \pm 195$ cal a BP (Praeg *et al.*, 2015). BRITICE-CHRONO further recovered a further series of nine cores from the Celtic Sea containing glacimarine sequences and, in one case, till from close to the shelf break (JC106-003VC; Fig. 1; Scourse *et al.*, 2019). The glacimarine facies have yielded a suite of five ^{14}C ages, ranging from $24\,280 \pm 230$ to $26\,991 \pm 350$ cal a BP ($\Delta R = 0$). It is not possible at present to identify whether this spread of ages incorporates multiple readvance phases or only a single advance–retreat phase, but the mean of the six ages available is 25.2 cal ka BP. This is within the error of the combined OSL and TCN ages from Scilly and indicates the extension of the ISIS as far as the continental shelf break some time prior to ~25.2 cal ka BP and initiation of deglaciation at that time.

Celtic Deep

Cores taken through sequences within the Celtic Sea have typically recovered thick Holocene sandy mud to mud sequences overlying a coarse, shelf gravel lag above an erosional unconformity cut through glacigenic mud sequences (Austin and Scourse, 1997; Scourse *et al.*, 2002; Furze *et al.*, 2014). BRITICE-CHRONO recovered two piston cores (JC106-051/052PC) supported by acoustic data from the Celtic Deep (Fig. 1; Lockhart *et al.*, 2018; Scourse *et al.*, 2019); these data indicate very similar sequences to those described previously. Furze *et al.* (2014) attribute the basal glacigenic muds to probable glacilacustrine rather than glacimarine conditions on the basis of their contained microflora and fauna, with the implication that deglaciation across the northern Celtic Sea might have been terrestrial rather than marine, a conclusion consistent with Tóth *et al.* (2020).

South and East Ireland

Before the BRITICE-CHRONO project, exposures of Irish Sea Till in coastal sections in southern Ireland had yielded ^{14}C and OSL data (Ó Cofaigh and Evans, 2001a,b, 2007; Ó Cofaigh *et al.*, 2012) indicating the flow of the ISIS after 26 cal ka BP westwards into the Celtic Sea and then onshore on exiting the constriction of St George's Channel, lending support to the notion of a piedmont lobe across the Celtic shelf. Ó Cofaigh *et al.* (2012) collected OSL ages for glacilacustrine and glacifluvial sediments overlying Irish Sea Till at Whiting Bay and Ballycroneen Strand constraining Irish Sea ice withdrawal

© 2021 The Authors *Journal of Quaternary Science* Published by John Wiley & Sons, Ltd.

10991417, 2021, 5, Downloaded from https://onlinelibrary.wiley.com/doi/10.1002/jqs.3313 by Ogs Trieste Istituto Nazionale, Wiley Online Library on [24/11/2023]. See the Terms and Conditions (https://onlinelibrary.wiley.com/terms-and-conditions) on Wiley Online Library for rules of use; OA articles are governed by the applicable Creative Commons License

from the coastline of southern Ireland to ~24 ka, and thus affirming a short-lived and rapid advance of the ISIS to maximum limits in the Celtic Sea. Further north and east, sedimentological and structural interpretation of the complex but undated glacitectonized sequences of the Screen Hills in southeast Ireland indicated deposition and thrusting during a series of readvance phases of the right lateral terrestrial margin of the marine-terminating ISIS within the ISB (Thomas and Summers, 1983, 1984; Thomas and Chiverrell, 2011). The structural framework of the Screen Hills complex provided a chronological template of readvance phases tested by a programme of OSL and TCN dating by BRITICE-CHRONO, in addition to the application of these techniques at other sites in southeastern and eastern Ireland.

A total of 13 OSL and 10 TCN determinations have been generated by BRITICE-CHRONO (Small *et al.*, 2018) that document the initially rapid retreat of the ISIS out of the Celtic Sea. Initial rates may have been as high as 300–600 m a^{-1}. It has been inferred that such rapid retreat here might be related to grounding line retreat across the nearby reverse slope of the Celtic Deep. The deepest part of the Celtic Deep is between −140 and −150 m and the adjacent Celtic Deep Southern Sill less than −80 m (Furze *et al.*, 2014). The data support the interpretation for a deceleration in retreat rate (26 m a^{-1}) followed by stabilization (3 m a^{-1}), indicated by the series of readvance phases between 23.3 and 22.9 ka in the Screen Hills sequence that are located in the topographic constriction of St George's Channel. Subsequent retreat northwards of this constriction after 22.9 ka along the normal slope of the ISB was then faster (~125–150 m a^{-1}) (Smedley *et al.*, 2017a; Small *et al.*, 2018).

Wales

Luminescence ages from deglacial sequences in Cardigan, southwest Wales, indicate the ISIS retreat potentially as early as ~26.7 ka (Glasser *et al.*, 2018). The Llŷn Peninsula in northwest Wales contains numerous ice-marginal morpho-sedimentary indicators of stepped retreat and readvance phases, notably morainal banks with thrust, stacked and tectonized sequences delineating inter-morainal basins (Thomas and Chiverrell, 2007). The Thomas and Chiverrell interpretation (2007) of this previously largely undated retreat sequence provided a morpho-stratigraphic template for tightly targeted OSL sampling of proglacial sequences and re-evaluation of existing TCN data within the BRITICE-CHRONO project (Smedley *et al.*, 2017b). This sector of the ISIS is characterized by topographic constriction, a reverse bed slope and changing widths of the former calving margin. The new data from Abermawr, Banc-y-Warren and Tonfanau have been integrated into a regional Bayesian model that indicates centennial-scale oscillatory behaviour of the ice front between 24 and 20 ka BP across a relatively short axial distance (~120 km) consistent with a slowing in the overall rate of ISIS retreat (Smedley *et al.*, 2017b).

English Midlands

Luminescence measurements on cobbles and sediments from glacifluvial sequences deposited by the terrestrial-terminating ISG, which extended into the English Midlands, indicate initial substantial advance reaching south Lancashire >30 ka and a maximum ice limit established ~26.5 ka in the vicinity of Bridgwalton and Seisdon (Fig. 1B; Chiverrell *et al.*, 2021). Extensive geomorphological mapping (Thomas, 1985, 1989; Thomas *et al.*, 2004; Thomas and Chiverrell, 2007) has demonstrated that this advance was sourced by ice from the Lake District, the northern Irish Sea and north Wales. Retreat ice margins facing towards a series of reverse bedrock slopes generated numerous ephemeral proglacial lakes that strongly conditioned the style of deglaciation which commenced at ~25.3 ka in the south; the ice margins pulled-back from the Cheshire lowlands into the eastern Irish Sea and Lancashire after 22.1 ± 1.1 ka.

Northern Irish Sea

A synthesis of offshore geological and geophysical data combined with TCN and OSL dating of glacigenic landforms and sediments in the northern Irish Sea, north Wales, Isle of Man and western Cumbria provides constraints on the timing and retreat pattern of the ISIS northwards once the discrete west and east components of the ISIS and ISG had deglaciated (Chiverrell *et al.*, 2018). This synthesis incorporated previously published ^{14}C ages on marine microfauna (McCabe *et al.*, 1998; McCabe *et al.*, 2007; McCabe, 2008; Ballantyne and Ó Cofaigh, 2017). As the retreating ice front escaped the topographic constriction of the central Irish Sea – Llŷn Peninsula, ice retreat accelerated at ~20 ka in response to this wider calving margin but slowed on reaching the Isle of Man as the ISIS stabilized and oscillated with a series of readvance phases. These generated the glacitectonized thrust stratigraphy characteristic of the Isle of Man sequence (Thomas and Summers, 1984; Thomas *et al.*, 2004) including components produced during the Scottish Readvance of ice margins. The new ages demonstrate that the Scottish Readvance occurred between 19.2 and 18.2 ka, earlier than previously suggested and not coincident with Heinrich Event 1 (Chiverrell *et al.*, 2018). The ISIS then retreated northwards towards the Southern Uplands of Scotland, with the Bayesian analysis showing deglaciation of the southern Solway Lowlands at ~15.5 ± 0.6 ka (Chiverrell *et al.*, 2018).

Materials and methods

The materials and methods used in the contributory investigations are included in detail in the individual papers reporting the findings, as listed above. New OSL ages developed for three sites in west Wales are presented here.

OSL geochronology

OSL dating determines the time elapsed since a mineral grain (typically quartz or K-feldspar) was last exposed to sunlight before burial (see Rhodes, 2011; Smedley, 2018). Because of exposure of the mineral grains to naturally occurring ionizing radiation, charge accumulates at defects within the crystal structure and builds up through time. The charge can be released in the laboratory by stimulating with light at a particular wavelength, and the energy liberated from this process produces light which can be detected at a different wavelength. This emission of light is called luminescence, and is the OSL signal measured from the sample. The OSL signal can be used to calculate the equivalent dose (D_e), a measure of the total ionizing radiation received by the sample during its period of burial. To determine an OSL age, D_e is divided by the environmental dose-rate (a measure of how much radiation the sample experiences per year) which combines the contributions from alpha, beta and gamma radiation, along with the cosmic dose-rate.

The new OSL ages reported in this paper were determined using measurements of the OSL signal from single grains of quartz. To calculate the environmental dose rate to the quartz

© 2021 The Authors *Journal of Quaternary Science* Published by John Wiley & Sons, Ltd.

10991417, 2021, 5, Downloaded from https://onlinelibrary.wiley.com/doi/10.1002/jqs.3313 by Ogs Trieste Istituto Nazionale, Wiley Online Library on [24/11/2023]. See the Terms and Conditions (https://onlinelibrary.wiley.com/terms-and-conditions) on Wiley Online Library for rules of use; OA articles are governed by the applicable Creative Commons License

grains, U, Th, K and Rb concentrations were measured on milled and homogenized bulk sediment samples using inductively coupled plasma mass spectrometry (ICP-MS) and atomic emission spectroscopy (ICP-AES) (Table 1). The beta dose-rates were calculated from the concentration of these radionuclides in each sample using the conversion factors of Guérin *et al.* (2011) and corrected for grain size and HF etching using the beta dose-rate attenuation factors of Guérin *et al.* (2012). Gamma dose-rates were determined in the field using *in situ* gamma spectrometry with a 2-inch-diameter NaI:Tl scintillator. Water contents were estimated considering the field and saturated water contents, and the environmental history for each sample. The dose-rate due to cosmic rays was calculated after Prescott and Hutton (1994). All dose rate calculations were undertaken using the Dose Rate and Age Calculator (DRAC; Durcan *et al.*, 2015).

Grains of quartz used for OSL measurements to determine equivalent doses (D_e) were isolated by treating each sample with a 10% (v/v) dilution of 37% HCl and with 20% (v/v) of H_2O_2 to remove carbonates and organics, respectively. Dry sieving then isolated the 212–250 μm diameter grains for all samples. Density separation using sodium polytungstate then provided the 2.62–2.70$^-$ g cm^{-3} (quartz-dominated) fractions, which were etched for 1 h in 40% hydrofluoric acid (HF) to remove the outer portion of the quartz grains that was affected by alpha irradiation and any contaminating feldspar. Grains were then washed in a 10% solution of HCl to remove any fluorides that may have been produced during the HF etch. Finally, grains of quartz were mounted on a 9.8-–mm-diameter aluminium single-grain disc for analysis, which contained a 10 by 10 grid of 300-μm-diameter holes.

All luminescence measurements were performed using a Risø TL/OSL DA-15 automated single-grain system equipped with a ^{90}Sr/^{90}Y beta source (Bøtter-Jensen *et al.*, 2003). Optical stimulation was performed for 1 s using a green laser at 125 °C and the OSL signal was detected through a 2.5-mm-thick U-340 filter and convex quartz lens placed in front of the photomultiplier tube. The first 0.1 s and final 0.2 s of stimulation were summed to calculate the initial and background OSL signals, respectively. A preheat plateau test performed on sample T4BANC02 was used to determine the preheat temperature (200 °C for 10 s) applied throughout the single aliquot regenerative dose (SAR) protocol (Murray and Wintle, 2000). The grains were accepted after applying the following screening criteria and accounting for the associated uncertainties: (i) whether the test dose response was greater than three sigma above the background, (ii) whether the test dose uncertainty was <20%, (iii) whether the recycling and OSL-IR depletion ratios were within the range of ratios 0.8–1.2, (iv) whether recuperation was <5% of the response from the largest regenerative dose and (v) whether the single-grain D_e values were not from a population of very low doses that were identified by the finite mixture model (FMM) to be inconsistent with the geological context of the sample (i.e. <1 ka). To assess the performance of the SAR protocol, dose–recovery experiments were performed on all the samples with the OSL signals bleached using blue light emitting diodes (LEDs). The samples gave dose recovery ratios within 10% of unity, showing that the SAR protocol used for analysis could accurately recover a known laboratory radiation dose and was therefore appropriate for these samples.

Bayesian methodology

Each of the geochronological methods employed to constrain ice retreat generates an age probability distribution, with each technique affected by method-specific limitations in their application (discussed above). Bayesian age modelling (Buck *et al.*, 1996; Bronk Ramsey, 2008) describes a group of approaches applied widely to integrated dating control for sediment sequences. The process refines the probability distributions for individual ages and relies on a series of ages that are presented as an order of events discerned independently of the chronology. The approach is routinely applied to sets of age measurements related by stratigraphy and governed by the principle of superposition, for example radiocarbon ages from lake or peat sequences (Bronk Ramsey, 2008). Bayesian modelling has been applied increasingly to spatially distributed geomorphological datasets where there is a single actor responsible for the relative order of events, for example the progression of fluvial terraces (Chiverrell *et al.*, 2009) and the retreat of glacial margins (e.g. Chiverrell *et al.*, 2013, 2018, 2020; Bradwell *et al.*, 2019). The deglaciation sequence for the ISIS and ISG as evidenced in the onshore and offshore geomorphology provides this hypothetical 'relative-order' of events for Bayesian modelling of the geochronological determinations (e.g. Chiverrell *et al.*, 2013). In the terminology of Bayesian chronological modelling this is the Prior model (e.g. Chiverrell *et al.*, 2013).

The Prior model for the ISIS extends with ice marginal retreat from maximum limits near the continental shelf break in the southern Celtic Sea through well-defined ice margin configurations identified on the sea floor and in the coastal zone of adjacent land masses through the ISB across the Isle of Man and stepping-back on to land in southwest Scotland (Ballantyne *et al.*, 2013; Praeg *et al.*, 2015; Chiverrell *et al.*, 2016; Smedley *et al.*, 2017a,b; Chiverrell *et al.*, 2018, 2020; Jenkins *et al.*, 2018; Small *et al.*, 2018; Wilson *et al.*, 2018; Ballantyne and Small, 2019; Scourse *et al.*, 2019). Two further published Bayesian models are included here; the Prior models for these were developed for (i) the largely terrestrial retreat sequence of the ISG from maximum limits in the English Midlands to the Lancashire coast (Chiverrell *et al.*, 2020), and (ii) the step-back of the ISIS from the western ISB into the northeast of Ireland (Chiverrell *et al.*, 2018). Together, these three Prior models describe the retreat dynamics for this sector

Table 1. Environmental dose-rates to grains of quartz, determined using ICP-MS and ICP-AES analysis and field gamma spectrometry. The chemical concentrations are presented to the appropriate decimal places according to the associated detection limit. The grain size for all samples was 212–250 μm. The water contents are expressed as a percentage of the mass of dry sediment. Dose-rates were calculated using the Dose Rate and Age Calculator (DRAC; Durcan *et al.*, 2015).

Sample	Depth (m)	Water content (%)	K (%)	Rb (p.p.m.)	U (p.p.m.)	Th (p.p.m.)	Beta dose-rate (Gy ka^{-1})	Gamma dose-rate (Gy ka^{-1})	Cosmic dose-rate (Gy ka^{-1})	Total dose-rate (Gy ka^{-1})
T4ABMW01	3	30 ± 5	1.1 ± 0.1	36.3 ± 3.6	1.03 ± 0.10	3.7 ± 0.4	0.7 ± 0.1	0.5 ± 0.1	0.1 ± 0.0	1.4 ± 0.1
T4BANC01	4	17 ± 5	0.7 ± 0.1	24.2 ± 2.4	0.99 ± 0.10	3.7 ± 0.4	0.6 ± 0.1	0.4 ± 0.0	0.1 ± 0.0	1.1 ± 0.1
T4BANC02	20	23 ± 5	0.8 ± 0.1	30.7 ± 3.1	0.79 ± 0.08	2.4 ± 0.2	0.6 ± 0.1	0.3 ± 0.0	0.1 ± 0.0	0.9 ± 0.1
T4TONF01	1	20 ± 5	2.3 ± 0.2	86.4 ± 8.6	1.95 ± 0.20	8.7 ± 0.9	1.7 ± 0.2	0.9 ± 0.1	0.2 ± 0.0	2.8 ± 0.2

© 2021 The Authors *Journal of Quaternary Science* Published by John Wiley & Sons, Ltd.

10991417, 2021, 5, Downloaded from https://onlinelibrary.wiley.com/doi/10.1002/jqs.3313 by Ogs Trieste Istituto Nazionale, Wiley Online Library on [24/11/2023]. See the Terms and Conditions (https://onlinelibrary.wiley.com/terms-and-conditions) on Wiley Online Library for rules of use; OA articles are governed by the applicable Creative Commons License

of the former BIIS with the exception of the retreat of ice into the mountainous interior of Wales which operated as a separate ice cap (McCarroll and Ballantyne, 2000; Patton *et al.*, 2013a,b,c; Hughes *et al.*, 2016).

Each Prior model was developed independently of the age information and included all geochronological samples according to procedures set out in Bronk Ramsey (2008, 2009a,b) and Bronk Ramsey and Lee (2013). Markov chain Monte Carlo (MCMC) sampling in the Bayesian analysis uses the Prior models and the likelihood (measured ages) probabilities for all samples to build distributions of possible solutions, thereby generating modelled probabilities termed posterior density estimates (1σ age ranges). The Bayesian models were coded in OxCal 4.3 (Bronk Ramsey and Lee, 2013) as Sequence models, and the Prior models were structured as a series of Phases that contain dating information grouped for retreat stage zones, each including sites that share relationships with the adjacent zones. Phases, unordered group of events/parameters in the OxCal nomenclature, are delimited by the Boundary command located in the code typically at well-defined ice margin limit positions and are termed Boundary Limits (BLs). The Boundary command in Sequence models generates modelled age probability distributions that here reflect the ages of those BLs, for the ISIS labelled BL1 to BL20, for the ISG in the English Midlands labelled E-BL1 to E-BL10 and for the step-back of ice into northeast Ireland labelled NI-BL1 to NI-BL7 (Fig. 1A). In summary, the Bayesian modelling uses uniform Phase Sequence models punctuated by Boundaries, and run to assess outliers in time using a scaling of 10^0 to 10^4 years using a Student's *t*-distribution to describe the outliers (Bronk Ramsey, 2009b).

Numerous iterations of the modelling were undertaken varying the outlier probabilities for individual age determinations to achieve overall model agreement indices exceeding the >60% threshold advocated by Bronk Ramsey (2009a). Outliers were given ultimately a probability scaling based on their fit within the model, thereby allocating probabilities of $p < 0.2$, $p < 0.5$, $p < 0.75$ and $p = 1$ (100%) on a scale of increasing outlier severity. Individual ages were assessed based on their fit both within an individual Phase and in the progression between Phases of the Sequence model. Bottlenecks in the modelling were handled by increasing iteratively the outlier probability for all ages in selected Phases until the model produced overall agreement, at which point agreement indices are produced for all ages individually. The statistical outliers identified by that process were not arbitrarily excluded but scrutinized for reasons explaining outlier behaviour either in the Prior model (e.g. the sample context) or in the measurement data (e.g. nuclide inheritance). Once outliers ($p = 1$; 100%) had been identified, the outlier probabilities were decreased for subsequent iterations, with this process-cycling continuing until the overall model agreement was >60%. Samples handled as outliers for the ISIS are detailed in later sections. Outlier handing for the English Midlands and northeast Ireland Sequence models are described in Chiverrell *et al.* (2018, 2021).

Results

Site descriptions and stratigraphy

Abermawr [51.969813, −5.0831921]

Abermawr is located on the north coast of Pembrokeshire (Fig. 1B), where Irish Sea ice has impinged on a north-draining catchment 4–5 km west of Fishguard. The sequence at Abermawr (McCarroll and Rijsdijk, 2003) shows Irish Sea glacial sediments overlying locally derived breccia and gravels. The glacigenic sequence is deformed and comprises Irish Sea till overlain by offlapping outwash sands and gravels. The offlapping upper flows represent melt-out, flow tills and paraglacial slope wash redistributing the glacial sediments. The Abermawr coastal exposures in July 2013 showed Irish Sea diamicton, incorporating thin channel fill outwash sands, which were sampled for T4ABMW01 (Fig. 2A). The OSL sample was taken from a ~0.1–0.15-m-thick unit composed of horizontally laminated fine to medium sand that appeared to form an ice proximal outwash channel fill (Fig. 2B).

Banc-y-warren [52.106176, −4.624386]

Banc-y-Warren (Fig. 1B) is an important site in the Quaternary geology of SW Wales and a listed Geological Conservation Review locality. Geomorphologically the site is one of a series of steep-sided conical low hills that rise ~50 m above the northern flanks of the lower Teifi valley. Various models have been proposed to explain the sedimentology through these mounds exposed for many years in extensive sand and gravel workings. These models vary from end-moraines (Charlesworth, 1929), to coalescing ice front deltas feeding into proglacial Lake Teifi with bottom-set sands and

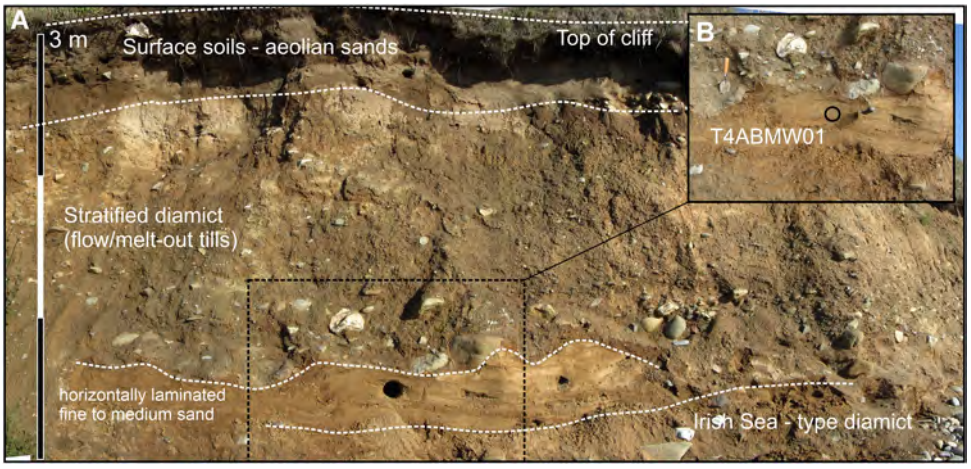

Figure 2. Coastal sections at the north end of Abermawr beach in July 2013 showing (A) the sequence of channelized horizontally laminated sands draped over an over-consolidated Irish Sea-type diamict and buried by more stratified diamictons interpreted as flow/melt-out tills giving way to paraglacial slope deposits. Inset (B) shows a close-up of OSL sample T4ABMW01. For full description and interpretation of these sections see McCarroll and Rijsdijk (2003). [Color figure can be viewed at wileyonlinelibrary.com].

© 2021 The Authors *Journal of Quaternary Science* Published by John Wiley & Sons, Ltd.

10991417, 2021, 5, Downloaded from https://onlinelibrary.wiley.com/doi/10.1002/jqs.3313 by Ogs Trieste Istituto Nazionale, Wiley Online Library on [24/11/2023]. See the Terms and Conditions (https://onlinelibrary.wiley.com/terms-and-conditions) on Wiley Online Library for rules of use; OA articles are governed by the applicable Creative Commons License

crossed-bedded gravels a foreset component (Jones, 1965; Helm and Roberts, 1975). Alternatively, the deposits have been interpreted as subaerial rather than subaqueous outwash spread on top of a down-wasting Irish Sea glacier (Allen, 1982). Hambrey *et al.* (2001) attribute the mounds of sand and gravel to recession of the Late Devensian Irish Sea ice margin with localized ice-bounded bodies of glaciofluvial sediment that accumulated on relatively high areas becoming ice-free on flanks of the lower Teifi valley and between remaining lobes of ice. In July 2013, the quarry at Banc-y-warren exposed the deposits of an ice-contact sandur system or kame terrace (Hambrey *et al.*, 2001); these yielded samples T4BANC01 and T4BANC02 (Fig. 3). OSL sample T4BANC01 was taken from high in the sequence in a unit of rippled fine and medium sand planar cross-sets reflecting relatively shallow back-bar environments, but adjacent to larger (metre-scale) trough cross-sets that probably indicate deeper water deltaic or channel systems (Fig. 3A). OSL sample T4BANC02 was taken from lower in the sequence from a unit of rippled fine to medium sand that also forms a larger (metre-scale) trough cross-sets probably deposited in deep channel systems (Fig. 3B).

Tonfanau [52.619176, −4.1253003]

The coastal cliffs at Tonfanau (central west Wales; Fig. 1B) comprise 2-km-long exposures of glacigenic sediments on the eastern margin of the ISB. Patton and Hambrey (2009) described a sequence recording the dynamics and deposition of sediments by both Welsh and Irish Sea ice, which included six lithofacies: diamicton, sandy gravel, well-rounded gravel, well-sorted sand, muddy sand and laminites. The lowermost units comprise a grey clast-poor muddy diamicton with sand and gravel in close association recording Welsh ice extending into Cardigan Bay. Higher in the sequence, sediments with a northern provenance bury the basal units, as a thick grounding-line fan complex developed fed by the ISIS flowing south and interacting with an ice-contact lake (Fig. 4A). Proximity of the ice margin is reflected in evidence for later overriding by the ISIS. These sediments are capped by a few metres of outwash (OLF-I to OLF-IV; Fig. 4B). OSL sample T4TONF01 was taken from high in the sequence (OLF-IV) in a unit of fine and medium sand in the upper sections of the grounding line fan complex (Fig. 4B,C). The sampled unit is part of a thicker succession of sand (OLF-III to OLF-IV) interpreted as subaerial outwash plain deposits by Patton and Hambrey (2009).

OSL data from west Wales sites

The OSL dating results for the four samples described above are presented in Tables 1 and 2, and each of the D_e distributions used to calculate ages are presented in Fig. 5. The D_e distributions determined for samples T4ABMW01 (Fig. 5a), T4BANC01 (Fig. 5b) and T4BANC02 (Fig. 5c) were asymmetrical, which is typical of sediments that were heterogeneously bleached before burial as is commonly observed for glacial sediments (e.g. Duller, 2008; Smedley *et al.*, 2017b). The minimum age model (MAM; Galbraith and Laslett, 1993; Galbraith *et al.*, 1999) is used to identify the well-bleached part of a heterogeneously bleached D_e distribution to determine an age, and it was therefore used to determine ages for these samples. A symmetrical D_e distribution was determined for sample T4TONF01 (Fig. 5d) and suggests that these grains were homogeneously bleached before burial; thus the central age model (CAM; Galbraith *et al.*, 1999) was used to determine this age and broadly calculates the weighted mean of a D_e distribution, accounting for the individual uncertainties of each datapoint. This difference in the scatter of the D_e data from these samples can be expressed numerically by calculating the overdispersion of each set of D_e values. Overdispersion is a measure of the scatter in the data beyond what would be expected from the uncertainties on individual D_e values, and much higher values are seen for the incompletely bleached samples (with values of 54–78%), than for the bleached sample with an overdispersion of 37% (Table 2).

To apply the MAM it is necessary to define the overdispersion that would be expected if the sample had been completely

Figure 3. The quarry sections at Banc-y-warren visited and sampled in July 2013 showing exposures in the upper 5–4 m of the sequence (A) and the lowest in sequence deposits then visible ~20 m below the surface (B). (A) T4BANC01 was sampled from horizontally (Sh) and planar cross-stratified (Sp) beds of rippled medium–fine sand, but adjacent to 1-m-scale trough cross-stratified sand (St) channel fill deposits. Inset (left) shows a close-up of OSL sample T4BANC01. (B) T4BANC02 was sampled from rippled fine to medium sand in stacked >1-m-scale trough cross-stratified sand (St) mostly likely deep-water channel fill deposits. Inset (right) shows a close-up of OSL sample T4BANC01. [Color figure can be viewed at wileyonlinelibrary.com].

© 2021 The Authors *Journal of Quaternary Science* Published by John Wiley & Sons, Ltd.

10991417, 2021, 5, Downloaded from https://onlinelibrary.wiley.com/doi/10.1002/jqs.3313 by Ogs Trieste Istituto Nazionale, Wiley Online Library on [24/11/2023]. See the Terms and Conditions (https://onlinelibrary.wiley.com/terms-and-conditions) on Wiley Online Library for rules of use; OA articles are governed by the applicable Creative Commons License

Figure 4. (A) Coastal section at Tonfanau sampled in December 2013 located 10 m north of the Log profile TON8 described by Patton and Hambrey (2009). The sequence comprises a steeply dipping basal package of ice-contact fan gravels with minor sand beds, buried by more horizontally bedded outwash lithofacies (OLF) OLF-I and OLF-II. Progressing up sequence, sand beds are increasingly dominant and OLF-III and IV dip more steeply to the south to south-west. (B) OLF-IV south-dipping beds of rippled coarse- to fine sand and the two samples collected. (C) Close-up of the sample T4TONF01 measured for OSL. For full description and interpretation of the Tonfanau sections see Patton and Hambrey (2009). [Color figure can be viewed at wileyonlinelibrary.com].

Table 2. Results from OSL dating, including the total number of grains analysed and the number of grains (*n*) that passed the screening criteria. The overdispersion (OD) from intrinsic sources of uncertainty was determined from dose-recovery (DR) experiments and combined in quadrature with OD from extrinsic sources (20%). The overdispersion values determined from intrinsic and extrinsic sources were rounded to the nearest 0.05 for consistency and used to determine the respective σ_b values for the three-parameter minimum age model (MAM).

					Overdispersion (OD)				
Site	Sample	Total grains	*n*	Age model	Natural (%)	DR (%)	σ_b	D_e (Gy)	Age (ka)
Abermawr	T4ABMW01	2000	48	MAM	54 ± 1	31	0.35	35.6 ± 6.8	25.2 ± 5.0
Banc-y-warren	T4BANC01	1600	63	MAM	78 ± 1	13	0.25	25.3 ± 3.7	22.1 ± 3.6
Banc-y-warren	T4BANC02	2700	55	MAM	61 ± 1	9	0.20	37.6 ± 4.7	39.6 ± 5.7
Tonfanau	T4TONF01	4000	33	CAM	37 ± 1	–	–	47.5 ± 3.6	17.2 ± 1.6

bleached at deposition. One approach to defining this overdispersion is to measure a well-bleached correlative of the sediments in question, but this is not possible for these sites. Instead, the approach used previously by Smedley *et al.* (2017b) was used. In this approach the overdispersion determined from the single-grain D_e dose recovery experiments, which quantified the amount of scatter caused by intrinsic sources of uncertainty, was added in quadrature to extrinsic overdispersion arising from external microdosimetry (estimated at 20%) to determine the value of σ_b used in application of the MAM. These σ_b values varied from 0.20 to 0.35 for the three samples where the MAM was used (Table 2).

The distribution of D_e values for the two samples from Banc-y-Warren are particularly scattered, and a large proportion of the grains do not appear to have been bleached at deposition, perhaps a result of short transport subaerially and deposition in deep water (as suggested by the sedimentology) where light exposure would be expected to be limited. However, in both cases it was possible to identify a population of grains for age determination (Fig. 5b,c, and ages in Table 2).

These four new OSL ages presented here constrain potentially three locations on the eastern margin of ISIS at a critical juncture during the passage northwards of ice margins between Ireland and Wales. They were selected to provide

© 2021 The Authors *Journal of Quaternary Science* Published by John Wiley & Sons, Ltd.

10991417, 2021, 5, Downloaded from https://onlinelibrary.wiley.com/doi/10.1002/jqs.3313 by Ogs Trieste Istituto Nazionale, Wiley Online Library on [24/11/2023]. See the Terms and Conditions (https://onlinelibrary.wiley.com/terms-and-conditions) on Wiley Online Library for rules of use; OA articles are governed by the applicable Creative Commons License

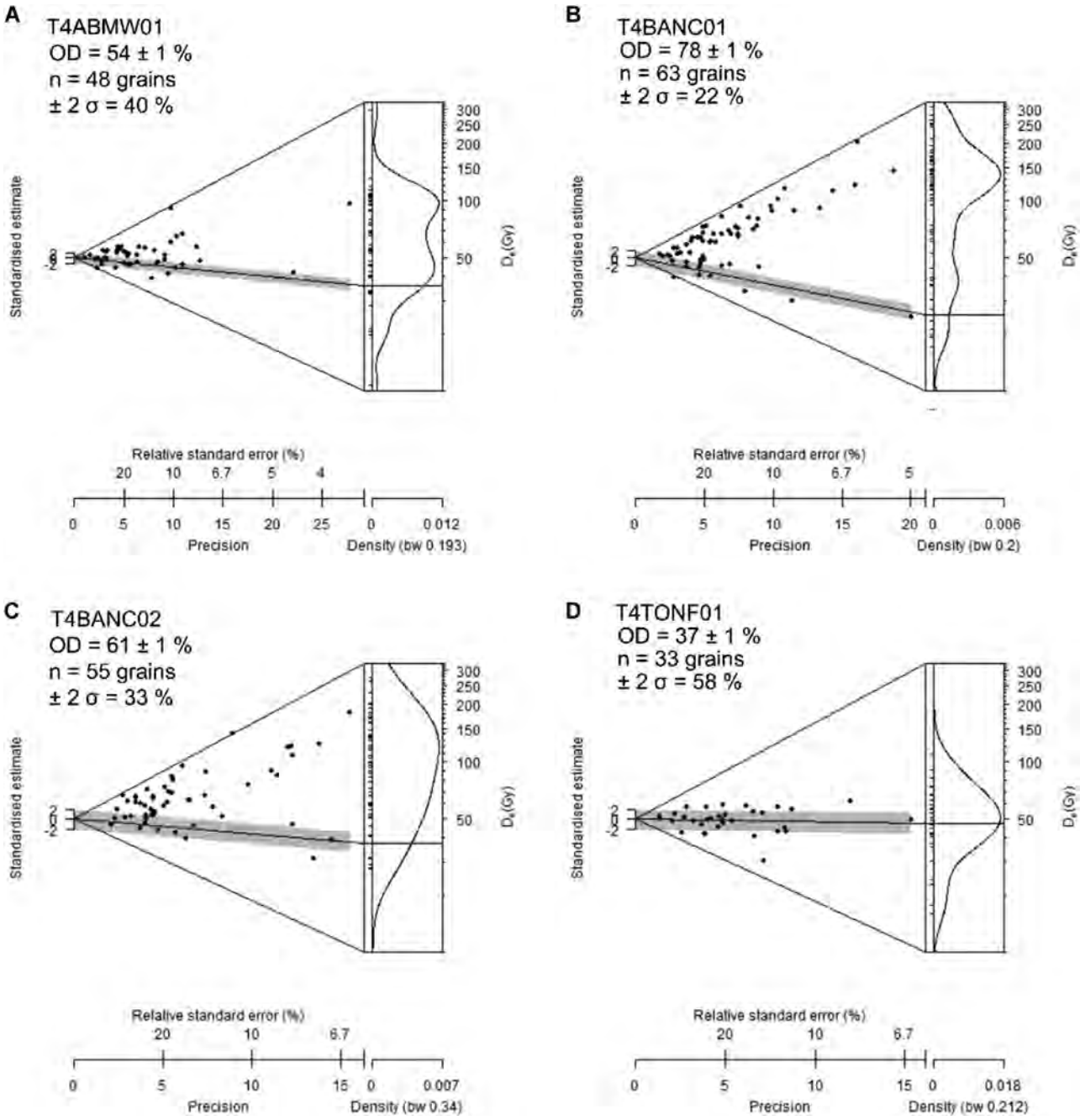

Figure 5. Abanico plots showing the single-grain D_e values determined from quartz. Data are presented in two forms to aid data interpretation, a radial plot and a probability density function. Each datapoint represents the D_e value determined from a single grain. The position on the *x*-axis indicates the precision of the individual D_e (more precisely known values are plotted to the right). The value of D_e for any given point can be read off by drawing a straight line from 0 on the primary *y*-axis (standardized estimate) through the datapoint to the secondary *y*-axis (D_e). Typically, samples well bleached before burial will have more symmetrical D_e distributions, in comparison to partially bleached sediments, which have asymmetrical D_e distributions. The line and grey shading represent either the CAM or MAM D_e value for that sample.

important constraints mirroring developing chronology in eastern Ireland (Small *et al.*, 2018), and for the eastern flank of ISIS to punctuate data from Scilly (Smedley *et al.*, 2017a) and the Llŷn Peninsula (northwest Wales) (Smedley *et al.*, 2017b). Furthest south of the three, a thin ice proximal outwash deposit at Abermawr (west Pembroke) yielded at age of 25.2 ± 5.0 ka, which considering the heterogeneous bleaching and the large age uncertainty is a good fit to the retreat sequence. Further north, Banc-y-Warren (north Pembroke) yielded a more equivocal chronology. The OSL age determined for T4BANC02 of 39.6 ± 5.79 ka came from low in the sequence and relatively deep-water channel or deltaic sands. This age pre-dates the build-up of ice in the Irish Sea sector (Scourse *et al.*, 2019; Chiverrell *et al.*, 2020) and thus is considered an inaccurate estimate of the time of deposition reflecting poor resetting of the OSL signal. Higher in the Banc-y-Warren sequence, though still heterogeneously bleached, these rippled fine and medium sands within trough cross-sets yielded an age of 22.1 ± 3.6 ka (T4BANC02). Both the Abermawr and the younger of the Banc-y-Warren ages post-date the chronology from Scilly, are similar in timing to ice margin retreat to the south coast of Ireland and pre-date ice margin retreat to the Llŷn Peninsula (Smedley *et al.*, 2017a,b; Small *et al.*, 2018).

Located broadly midway between Pembroke and the Llŷn Peninsula, the grounding-line fan complex at Tonfanau developed in an ice-contact lake between Welsh and Irish Sea ice (Patton and Hambrey, 2009). That interplay of ice

© 2021 The Authors *Journal of Quaternary Science* Published by John Wiley & Sons, Ltd.

10991417, 2021, 5, Downloaded from https://onlinelibrary.wiley.com/doi/10.1002/jqs.3313 by Ogs Trieste Istituto Nazionale, Wiley Online Library on [24/11/2023]. See the Terms and Conditions (https://onlinelibrary.wiley.com/terms-and-conditions) on Wiley Online Library for rules of use; OA articles are governed by the applicable Creative Commons License

masses, coupled with evidence for later overriding by Irish Sea ice, suggest a setting ideal for recording retreat of ISIS. Notwithstanding the homogeneous bleaching, the age of the 17.2 ± 1.6 ka (T4TONF01) is young compared with the well-constrained ice margin retreat chronology across the Llŷn Peninsula (Smedley *et al.*, 2017b). Constrained by the limited availability of suitable sand units, the sampling targeted sand units in the uppermost sandur deposit above the gravel-dominated proglacial fan wedges. It is possible that the unit sampled reflects either a late-stage subaerial sandur fed by Welsh ice or fluvial remobilization of the deposits under the periglacial conditions that Patton and Hambrey (2009) attribute to the uppermost muddy sand units at the location. In either case, the OSL age provides a minimum age on the passage northwards of Irish Sea ice margins.

Bayesian analysis modelling of ice retreat

Bayesian age modelling (Bronk Ramsey, 2009a) of the dating control for the ISIS provides a basis for calculating the timing for the advance and then retreat northeast and north through the Celtic and the ISB to the mountains of SW Scotland. The length and complexity of the prior model for the ISIS, coupled with an inherent scatter of using many age determinations, rendered obtaining a conformable agreement challenging. The model has therefore been broken into two sub-models, describing the south and north sectors respectively and including a zone of overlap where the Phases are included in both models (Fig. 6A; Table 3). The models have overall agreement indices of 120% for the south and 98% for the north, both exceeding the >60% threshold advocated by Bronk Ramsey (2009a). The iterative approach to assessing outliers, as described previously, resulted in a total of 28 out of the 93 age determinations being identified as absolute outliers (Table 3), with the remaining 65 receiving a variable outlier scaling of $p < 0.2$, $p < 0.5$ and $p < 0.75$ based on increasing outlier severity as prescribed by the model. Out of the 28 total outliers, six TCN ages on the Isle of Man and in western Cumbria are unconformable as they constrain ice sheet lowering (thinning) rather than ice marginal retreat (Chiverrell *et al.*, 2018). Nine further TCN ages were treated as outliers ($p = 1$); seven of these ages are unconformable on the basis of being 'too old'. TCN ages that are older than the true age of deglaciation are interpreted as reflecting nuclide inheritance. In some cases (e.g. TRE01, T4SCI02) this is obvious as the apparent exposure ages pre-date build-up of the BIIS (e.g. Brown *et al.*, 2007). Other samples (e.g. T4CSP02) have apparent ages that are only slightly older than the modelled deglaciation age but are still unconformable within the broader context of the prior model. Similarly, two 'too young' ages probably reflect post-depositional modification of boulders; T4CSP01, for example, is incorporated into a field boundary and has thus potentially been moved. Five ^{14}C ages are older than other members in a Phase of ages indicating marine fauna reworked into younger sediments, whereas the younger members of the Phase provide better constraint on the timing of deglaciation. Eight OSL ages were treated as outliers ($p = 1$), with two reflecting the sampling of units younger than deglaciation (e.g. at Battery, Isles of Scilly; Smedley *et al.*, 2017a) and six where other samples suggest poor resetting of the OSL signal. Throughout, all outlier samples were identified as outliers in the iterations of the Bayesian modelling and were not excluded subjectively. The Boundary ages constraining the retreat of ice margins were derived from the modelling (Fig. 6), with the zone of overlap using an average of the south and north modelled ages and uncertainties. In subsequent sections, italics denote the posterior density estimates or modelled ages derived from the Bayesian modelling to distinguish them from the unmodelled ages obtained directly for individual samples. Details on the Bayesian age modelling for the ISG and step-back of ice from the western ISB into the northeast of Ireland are provided in Chiverrell *et al.* (2020) and Chiverrell *et al.* (2018) respectively.

Basal constraint on ice advance in the Irish-Celtic Sea sector is provided by dated evidence for ice-free conditions in several locations. Four Ashes in the English Midlands (Staffordshire) yielded ^{14}C ages of around 34.6 ± 0.8 cal ka BP (Morgan, 1973) with additional OSL ages of around 27.8 ± 2.6 ka reported from further north at Dowkabottom (Lancashire; Telfer *et al.*, 2009). The Four Ashes ages are similar to equivalent dating of ice-free conditions at around 34.4 ± 1.8 cal ka BP based on ^{14}C ages from Sourlie on the Ayrshire coast in the feeder zone to ice in the North Channel (Finlayson *et al.*, 2010, 2014). Further east in central Scotland equivalent organic-rich sediments spanning 39.8–32.8 ka BP have been identified at Balglass Burn (north of Glasgow; Brown *et al.*, 2007); these sites are in the central sector of the former BIIS and provide important constraint on ice sheet build-up. Further constraint on the build-up of ice in the Irish Sea sector is provided by a cluster of OSL ages around 29.9 ± 1.2 ka from Lydiate Lane Quarry, which constrains the expansion of ice in the north ISB and extension into south Lancashire (Chiverrell *et al.*, 2021). The Four Ashes and Lydiate Lane ages have been incorporated into the Bayesian model for the Irish Sea Glacier (Fig. 6C), but they apply in a wider Irish Sea context recording a substantial build up and expansion of ice into the central Irish Sea by *28.3 ± 1.4 ka*. The retreat stages indicated by the Bayesian modelling are shown in Fig. 7.

Discussion

Celtic Sea and Celtic Deep

The maximum extension of the ISIS to the shelf break in the south Celtic Sea is well dated by TCN and OSL from Scilly and ^{14}C-dated fauna from glacimarine facies overlying subglacial diamict constraining the initial pull-back in the south Celtic Sea, all overlapping within uncertainties. These ages constrain the timing for the maximum extension of the ISIS (Fig. 7) near the continental shelf break to *25.6 ± 0.5 ka* (BL1) and the initial pullback of ice margins to *25.3 ± 0.2 ka* (BL2). Although probably integrating across pulses of ice margin advance, still-stand and retreat, the expansion phase amounts to a net axial advance of the ice stream of ~150 m a^{-1}. The Bayesian modelling has calculated modelled age probability distributions for the ISIS limits that show substantial changes in the pace of retreat, vacating the Celtic Sea rapidly between *25.3 ± 0.2 ka* (BL2) and *24.7 ± 0.2 ka* (BL4) at rates between 230 and 650 m a^{-1}. The rapid advance of the ISIS and high discharge of icebergs associated during the rapid retreat probably required high velocities in the ice stream, which is consistent with sea floor geomorphological indicators of fast flow in the central ISB, where a field of megascale glacial lineations are aligned NNE–SSW and axial parallel to ice flow towards the Celtic Sea evidence ice streaming (Van Landeghem and Chiverrell, 2020).

The glacimarine sequences of the Celtic Sea are in many cases, though not all, highly deformed and contorted, and are characterized by high values of undrained shear strength as measured by shear vane (Lockhart *et al.*, 2018; Scourse *et al.*, 2019). The geotechnical properties of these sequences are difficult to explain without subsequent overriding and glacitectonism as a result of ice readvance (Lockhart, 2019) and their distribution identifies the specific sector of the Celtic

© 2021 The Authors *Journal of Quaternary Science* Published by John Wiley & Sons, Ltd.

10991417, 2021, 5, Downloaded from https://onlinelibrary.wiley.com/doi/10.1002/jqs.3313 by Ogs Trieste Istituto Nazionale, Wiley Online Library on [24/11/2023]. See the Terms and Conditions (https://onlinelibrary.wiley.com/terms-and-conditions) on Wiley Online Library for rules of use; OA articles are governed by the applicable Creative Commons License

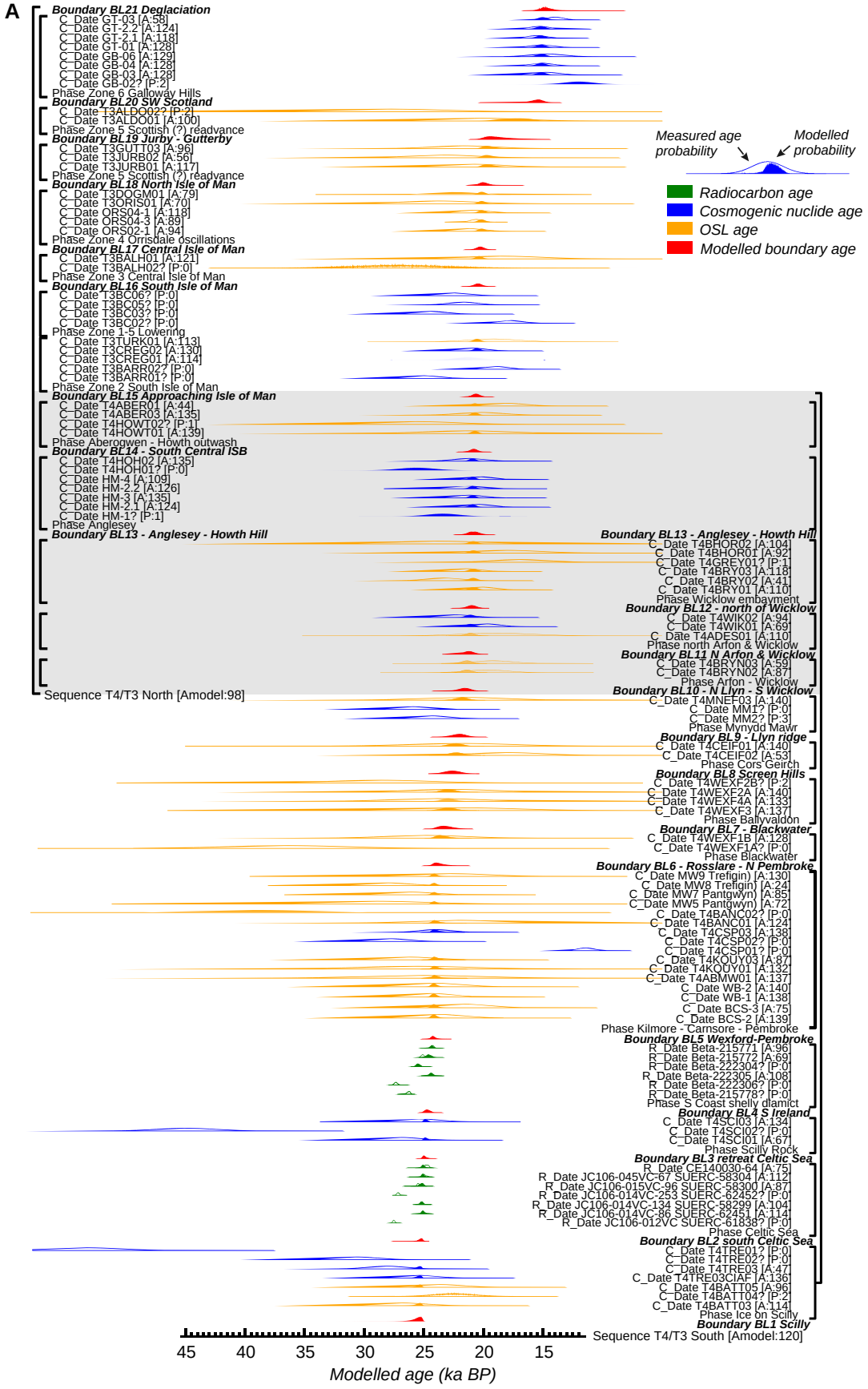

Figure 6. Bayesian chronosequence age-model output of dating constraints using OxCal 4.3 for (A) ISIS, (B) retreat into the northeast of Ireland (Chiverrell *et al.*, 2018) and (C) ISG (English Midlands) (Chiverrell *et al.*, 2020). The model structure shown uses OxCal brackets (left) and keywords that define the relative order of events (Bronk Ramsey, 2009a). Each original distribution (hollow) represents the relative probability of each age estimate with posterior density estimate (solid) generated by the modelling. Shown are ^{14}C ages (R_Date, green), OSL ages (C_Date, orange), cosmogenic nuclide ages (C_Date, blue) and modelled boundary ages (red). Outliers are denoted by '?' and their probability (p) of being an outlier indicated by low values, e.g. <5 (95% confidence). Model agreement indices for individual ages show their fit to the model with >60% the widely used threshold for 'good' fit (Bronk Ramsey, 2009b). [Color figure can be viewed at wileyonlinelibrary.com].

© 2021 The Authors *Journal of Quaternary Science* Published by John Wiley & Sons, Ltd.

10991417, 2021, 5, Downloaded from https://onlinelibrary.wiley.com/doi/10.1002/jqs.3313 by Ogs Trieste Istituto Nazionale, Wiley Online Library on [24/11/2023]. See the Terms and Conditions (https://onlinelibrary.wiley.com/terms-and-conditions) on Wiley Online Library for rules of use; OA articles are governed by the applicable Creative Commons License

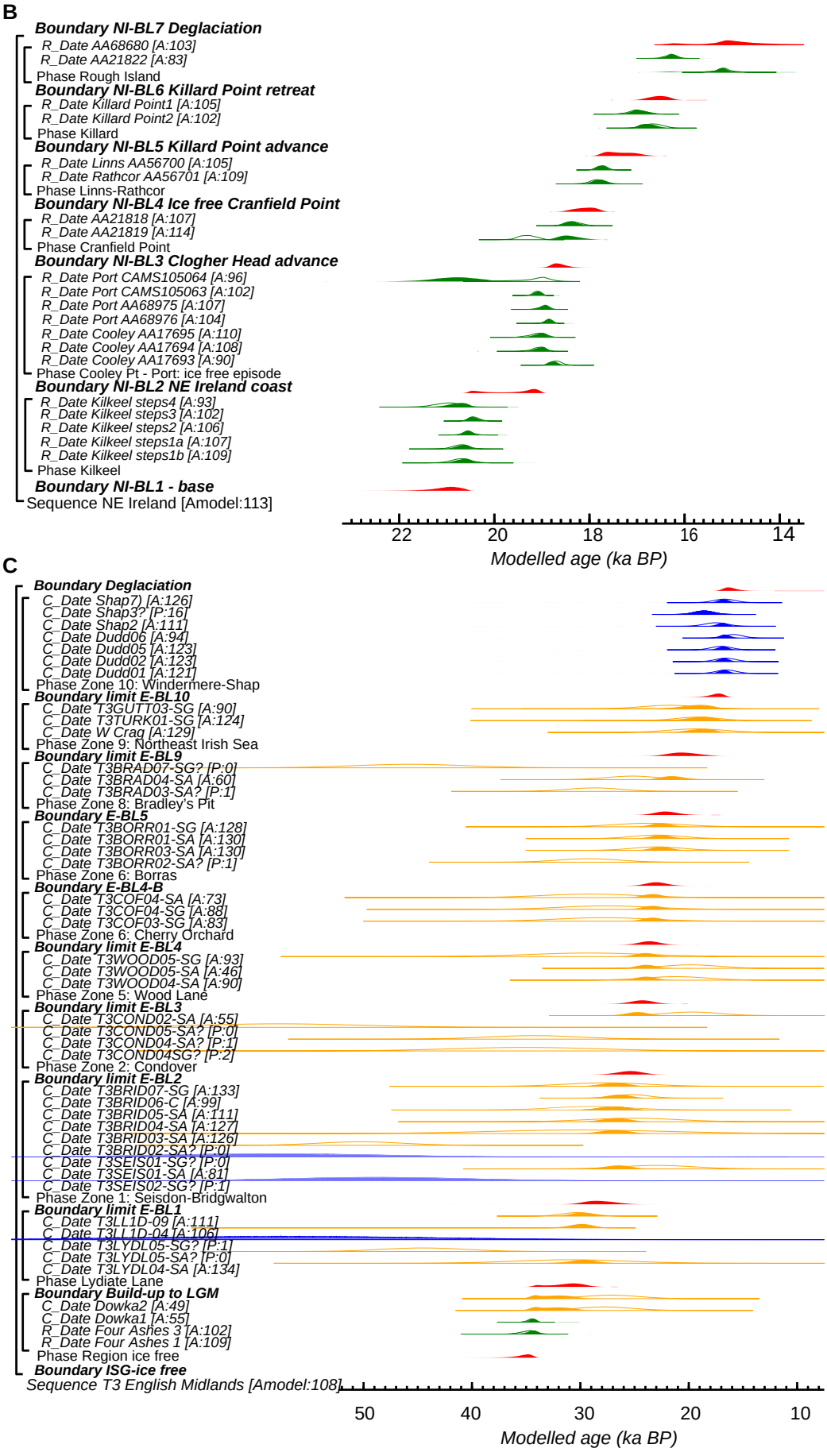

Figure 6. Continued

10991417, 2021, 5, Downloaded from https://onlinelibrary.wiley.com/doi/10.1002/jqs.3313 by Ogs Trieste Istituto Nazionale, Wiley Online Library on [24/11/2023]. See the Terms and Conditions (https://onlinelibrary.wiley.com/terms-and-conditions) on Wiley Online Library for rules of use; OA articles are governed by the applicable Creative Commons License

Table 3. The modelled boundary limit ages for the ISIS, alongside Bayesian model boundary ages for the ISG (Chiverrell *et al.*, 2021) and retreat of ice margins into the north of Ireland (Chiverrell *et al.*, 2018). All boundary ages are expressed as ±1σ. Ages marked with an asterisk are identified as outliers that did not influence the modelled outputs. Model structures show the named Phases in the Bayesian age models and groups of dating information for the three models. Boundary ages are spaced vertically to highlight correlation of timing between sectors.

Irish Sea Ice Stream					Irish Sea Glacier					Retreat from N Irish Sea Basin				
Model structure	Age information	Unmodelled age	*Modelled age*	*Boundary age*	Model structure	Age information	Unmodelled age	*Modelled age*	*Bound. age*	Model structure	Age information	Unmodelled age	*Modelled age*	*Boundary age*
					E Ice free				*35.2 ± 4.5*					
					Ice free pre-MIS 2 LGM	R_Date Four Ashes 1	30.7 ± 0.8	*34.4 ± 1.7*						
						R_Date Four Ashes 3	30.5 ± 0.4	*34.4 ± 4.1*						
						C_Date Dowka1	27.8 ± 2.6	*32.6 ± 1.7*						
						C_Date Dowka2	27.2 ± 2.6	*32.5 ± 1.8*						
					E Build-up Pre-LGM Ice buildup				*31.2 ± 1.7*					
						C_Date T3LYDL04-SA	30.9 ± 5.2	*29.8 ± 1.5*						
BL1				*25.6 ± 0.5*		C_Date T3LYDL05-SA	44.5 ± 3.9	*						
Ice on Scilly	T4BATT03	26.8 ± 2.0	*25.4 ± 0.4*			C_Date T3LYDL05-SG	57.2 ± 13.1	*						
	T4BATT04	22.5 ± 1.8	*			C_Date T3LL1D-04	30.2 ± 1.1	*29.9 ± 1.1*						
	T4BATT05	23.7 ± 2.0	*25.4 ± 0.3*			C_Date T3LL1D-09	30.3 ± 1.7	*29.9 ± 1.1*						
	T4TRE03ciaf	25.4 ± 1.5	*25.4 ± 0.3*		E BL1				*28.3 ± 1.4*					
	T4TRE03	28.1 ± 1.6	*25.5 ± 0.4*		Seisdon-Bridgwalton	C_Date T3SEIS02-SG	48.8 ± 8.4	*						
	T4TRE02	30.7 ± 1.8	*			C_Date T3SEIS01-SA	22.9 ± 3.4	*26.6 ± 1.2*						
	T4TRE01	53.4 ± 3.0	*			C_Date T3SEIS01-SG	58.5 ± 10.5	*						
BL2				*25.3 ± 0.2*		C_Date T3BRID02-SA	50.3 ± 3.9	*						
Celtic Sea	JC106-012VC SUERC-61838	23.3 ± 0.08	*			C_Date T3BRID03-SA	30.1 ± 8.0	*26.9 ± 1.3*						
	JC106-014VC-86 SUERC-62451	20.7 ± 0.06	*25.1 ± 0.1*			C_Date T3BRID04-SA	25.2 ± 4.1	*26.7 ± 1.3*						
	JC106-014VC-134 SUERC-58299	20.9 ± 0.05	*25.1 ± 0.1*			C_Date T3BRID05-SA	29.0 ± 3.5	*26.9 ± 1.3*						
	JC106-014VC-253 SUERC-62452	22.8 ± 0.07	*			C_Date T3BRID06-C	25.3 ± 1.6	*26.4 ± 1.1*						
	JC106-015VC-96 SUERC-58300	21.1±0.06	*25.2 ± 0.2*			C_Date T3BRID07-SG	27.6 ± 3.8	*26.8 ± 1.3*						
	JC106-045VC-67	20.7 ± 0.07	*25.1 ± 0.1*		E BL2				*25.4 ± 1.2*					

(*Continued*)

© 2021 The Authors *Journal of Quaternary Science* Published by John Wiley & Sons, Ltd.

10991417, 2021, 5, Downloaded from https://onlinelibrary.wiley.com/doi/10.1002/jqs.3313 by Ogs Trieste Istituto Nazionale, Wiley Online Library on [24/11/2023]. See the Terms and Conditions (https://onlinelibrary.wiley.com/terms-and-conditions) on Wiley Online Library for rules of use; OA articles are governed by the applicable Creative Commons License

Table 3. (*Continued*)

Irish Sea Ice Stream					Irish Sea Glacier					Retreat from N Irish Sea Basin				
Model structure	Age information	Unmodelled age	*Modelled age*	*Boundary age*	Model structure	Age information	Unmodelled age	*Modelled age*	*Boundary age*	Model structure	Age information	Unmodelled age	*Modelled age*	*Boundary age*
	SUERC-58304 CE140030-64	20.6 ± 0.08	*25.1 ± 0.1*		Glacial Lakes	C_Date T3COND04SG	35.1 ± 6.8	*						
BL3				*25 ± 0.1*	Newport - Severn	C_Date T3COND04-SA	34.3 ± 4.3	*						
Ice on Scilly	T4SCI01	26.9 ± 1.6	*24.8 ± 0.2*			C_Date T3COND05-SA	57.8 ± 7.5	*						
	T4SCI02	45.0 ± 2.5	*			C_Date T3COND02-SA	19.7 ± 2.5	*24.8 ± 1.1*						
	T4SCI03	25.3 ± 1.6	*24.8 ± 0.2*											
BL4				*24.7 ± 0.2*										
Ardmore,	Beta-215778	22.1 ± 0.09	*											
Whiting,	Beta-222306	23.0 ± 0.15	*											
Garryvoe	Beta-222305	20.3 ± 0.12	*24.5 ± 0.2*											
	Beta-222304	21.1 ± 0.13	*											
	Beta-215772	20.8 ± 0.08	*24.6 ± 0.2*											
	Beta-215771	20.2 ± 0.07	*24.4 ± 0.2*											
BL5				*24.3 ± 0.2*										
Watwerford -	T4ABMW01	25.2 ± 5.0	*24.2 ± 0.3*											
Kilmore -	T4KQUY01	25.7 ± 4.7	*24.2 ± 0.3*											
Carnsore -	T4KQUY03	26.2 ± 2.2	*24.2 ± 0.3*											
Pembroke	T4CSP01	11.4 ± 0.7	*		E BL3				*24.3 ± 1*					
	T4CSP02	27.8 ± 1.5	*		Oswestry-Whitchurch moraine									
	T4CSP03	24.0 ± 1.3	*24.2 ± 0.3*			C_Date T3WOOD04-SA	21.2 ± 2.9	*24 ± 1*						
	T4BANC01	22.2 ± 3.5	*24.2 ± 0.3*			C_Date T3WOOD05-SA	19.8 ± 2.6	*23.9 ± 1*						
	T4BANC02	39.6 ± 5.5	*			C_Date T3WOOD05-SG	29.2 ± 5.4	*24 ± 1*						
	MW5 Pantgwyn	29.1 ± 4.2	*24.2 ± 0.3*											
	MW7 Pantgwyn	26.2 ± 2.0	*24.2 ± 0.3*											
	MW8 Trefigin	28.1 ± 1.9	*24.2 ± 0.3*											
	MW9 Trefigin	22.8 ± 3.2	*24.2 ± 0.3*											
	Ballycroneen BCS-2	23.8 ± 2.1	*24.1 ± 0.3*		E BL4-A				*23.7 ± 1*					
	Ballycroneen BCS-3	21.6 ± 2.1	*24.1 ± 0.3*		Lake Delamere	C_Date T3COF03-SG	27.9 ± 2.8	*23.3 ± 1*						

(*Continued*)

© 2021 The Authors *Journal of Quaternary Science* Published by John Wiley & Sons, Ltd.

10991417, 2021, 5, Downloaded from https://onlinelibrary.wiley.com/doi/10.1002/jqs.3313 by Ogs Trieste Istituto Nazionale, Wiley Online Library on [24/11/2023]. See the Terms and Conditions (https://onlinelibrary.wiley.com/terms-and-conditions) on Wiley Online Library for rules of use; OA articles are governed by the applicable Creative Commons License

Table 3. (*Continued*)

Irish Sea Ice Stream					Irish Sea Glacier					Retreat from N Irish Sea Basin				
Model structure	Age information	Unmodelled age	*Modelled age*	*Boundary age*	Model structure	Age information	Unmodelled age	*Modelled age*	*Boundary age*	Model structure	Age information	Unmodelled age	*Modelled age*	*Boundary age*
	Whiting Bay WB-1	24.4 ± 1.8	*24.1 ± 0.3*			C_Date T3COF04-SG	27.6 ± 4.2	*23.3 ± 1*						
	Whiting Bay WB-2	24.2 ± 2.3	*24.1 ± 0.3*			C_Date T3COF04-SA	29.1 ± 4.3	*23.3 ± 1*						
BL6				*24.0 ± 0.4*	E BL4-B				*23 ± 1*					
Blackwater	T4WEXF1A	37.1 ± 5.0	*		Glacial Lake Bangor	C_Date T3BORR02-SA	29.2 ± 2.8	*						
	T4WEXF1B	24.9 ± 3.3	*23.7 ± 0.5*			C_Date T3BORR03-SA	22.9 ± 2.3	*22.6 ± 1*						
BL7				*23.4 ± 0.6*		C_Date T3BORR01-SA	22.9 ± 2.3	*22.6 ± 1*						
Ballyvaldon	T4WEXF3	21.8 ± 4.7	*23 ± 0.6*			C_Date T3BORR01-SG	23.7 ± 3.2	*22.6 ± 1*						
	T4WEXF4A	24.0 ± 3.7	*23.1 ± 0.6*											
	T4WEXF2A	22.7 ± 3.7	*23 ± 0.6*		E BL5				*22.1 ± 1.1*					
	T4WEXF2B	28.7 ± 4.2	*		North Ribble	C_Date T3BRAD03-SA	28.7 ± 2.5	*						
BL8				*22.7 ± 0.6*		C_Date T3BRAD04-SA	25.2 ± 2.3	*21.5 ± 1.1*						
Cors Geirch	T4CEIF02	18.0 ± 3.0	*22.4 ± 0.6*			C_Date T3BRAD07-SG	45.7 ± 5.2	*						
	T4CEIF01	21.9 ± 4.4	*22.4 ± 0.6*											
BL9				*22.1 ± 0.6*										
Mynydd Mawr	MM2	24.3 ± 1.4	*											
	MM1	26.0 ± 1.4	*											
	T4MNEF03	21.8 ± 3.7	*21.9 ± 0.5*											
BL10				*21.6 ± 0.5*										
Arfon - Wicklow	T4BRYN02	19.7 ± 1.7	*21.4 ± 0.4*											
	T4BRYN03	19.2 ± 1.6	*21.4 ± 0.4*											
BL11				*21.3 ± 0.4*										
Arfon & Wicklow	T4ADES01	18.9 ± 3.1	*21.1 ± 0.4*											
	T4WIK01	19.7 ± 1.1	*21.1 ± 0.4*											
	T4WIK02	22.3 ± 1.3	*21.1 ± 0.4*											
BL12				*21 ± 0.4*										
Wicklow embayment	T4BRY01	20.1 ± 1.1	*20.9 ± 0.3*											
	T4BRY02	23.3 ± 1.4	*20.9 ± 0.3*											
	T4BRY03	21.5 ± 1.2	*20.9 ± 0.3*							BL NE1 Kilkeel				*21 ± 0.4*
	T4GREY01	16.9 ± 2.3	*								R_Date Kilkeel steps1b	17.2 ± 0.16	*20.6 ± 0.2*	

(*Continued*)

© 2021 The Authors *Journal of Quaternary Science* Published by John Wiley & Sons, Ltd.

10991417, 2021, 5, Downloaded from https://onlinelibrary.wiley.com/doi/10.1002/jqs.3313 by Ogs Trieste Istituto Nazionale, Wiley Online Library on [24/11/2023]. See the Terms and Conditions (https://onlinelibrary.wiley.com/terms-and-conditions) on Wiley Online Library for rules of use; OA articles are governed by the applicable Creative Commons License

Table 3. (*Continued*)

Irish Sea Ice Stream					Irish Sea Glacier					Retreat from N Irish Sea Basin				
Model structure	Age information	Unmodelled age	*Modelled age*	*Boundary age*	Model structure	Age information	Unmodelled age	*Modelled age*	*Boundary age*	Model structure	Age information	Unmodelled age	*Modelled age*	*Boundary age*
	T4BHOR01	18.1 ± 2.9	*20.9 ± 0.3*								R_Date Kilkeel steps1a	17.2 ± 0.13	*20.7 ± 0.2*	
	T4BHOR02	24.0 ± 4.0	*20.9 ± 0.3*								R_Date Kilkeel steps2	17.0 ± 0.07	*20.6 ± 0.1*	
BL13				*20.9 ± 0.3*							R_Date Kilkeel steps3	16.9 ± 0.07	*20.5 ± 0.1*	
Anglesey	HM-1	23.4 ± 1.3	*								R_Date Kilkeel steps4	17.3 ± 0.19	*20.8 ± 0.2*	
	HM-2.1	20.4 ± 1.1	*20.9 ± 0.3*											
	HM-3	21.2 ± 1.2	*20.9 ± 0.3*											
	HM-2.2	21.5 ± 1.3	*20.9 ± 0.3*											
	HM-4	20.2 ± 1.1	*20.9 ± 0.3*											
	T4HOH01	25.6 ± 1.5	*											
	T4HOH02	21.2 ± 1.3	*20.9 ± 0.3*											
BL14				*20.8 ± 0.3*										
Aberogwen - Howth outwash	T4HOWT01	21.4 ± 3.6	*20.7 ± 0.3*		E BL9 Lancs - IoM - Cumbria				*20.6 ± 1.3*					
	T4HOWT02	25.6 ± 3.3	*			C_Date W Crag	19.3 ± 2.6	*18.9 ± 1.2*						
	T4ABER03	20.2 ± 1.9	*20.7 ± 0.3*			C_Date T3TURK01-SG	19.2 ± 2.0	*18.9 ± 1.1*						
	T4ABER01	18.1 ± 1.6	*20.7 ± 0.3*			C_Date T3GUTT03-SG	21.7 ± 2.6	*19.2 ± 1.3*						
BL15				*20.6 ± 0.3*										
South Isle of Man	T3BARR01	25.0 ± 1.3	*											
	T3BARR02	18.9 ± 1.0	*											
	T3CREG01	21.3 ± 1.2	*20.5 ± 0.3*											
	T3CREG02	20.9 ± 1.1	*20.5 ± 0.3*											
	T3TURK01	19.2 ± 2.0	*20.5 ± 0.3*											
Lowering Manx-Lakes	T3BC02	17.7 ± 1.0	*											
	T3BC03	24.2 ± 1.3	*											
	T3BC05	21.7 ± 1.2	*											
	T3BC06	22.4 ± 1.3	*											
BL16				*20.4 ± 0.3*										
Central Isle of Man	T3BALH02	27.1 ± 3.8	*											
	T3BALH01	18.5 ± 3.3	*20.4 ± 0.3*											
BL17				*20.3 ± 0.3*										
Orrisdale	ORS02-1	21.2 ± 1.2	*20.1 ± 0.3*											

(*Continued*)

© 2021 The Authors *Journal of Quaternary Science* Published by John Wiley & Sons, Ltd.

10991417, 2021, 5, Downloaded from https://onlinelibrary.wiley.com/doi/10.1002/jqs.3313 by Ogs Trieste Istituto Nazionale, Wiley Online Library on [24/11/2023]. See the Terms and Conditions (https://onlinelibrary.wiley.com/terms-and-conditions) on Wiley Online Library for rules of use; OA articles are governed by the applicable Creative Commons License

Table 3. (*Continued*)

Irish Sea Ice Stream					Irish Sea Glacier					Retreat from N Irish Sea Basin				
Model structure	Age information	Unmodelled age	*Modelled age*	*Boundary age*	Model structure	Age information	Unmodelled age	*Modelled age*	*Boundary age*	Model structure	Age information	Unmodelled age	*Modelled age*	*Boundary age*
oscillations	ORS04-3	20.6 ± 0.5	*20.1 ± 0.3*							BL NE2				*19.5 ± 0.5*
	ORS04-1	20.8 ± 1.2	*20.1 ± 0.3*							Cooley Pt - Port	R_Date Cooley AA17693	15.4 ± 0.11	*18.8 ± 0.1*	
	T3ORIS01	23.8 ± 3.1	*20.1 ± 0.3*								R_Date Cooley AA17694	15.8 ± 0.11	*19 ± 0.1*	
	T3DOGM01	22.5 ± 2.2	*20.1 ± 0.3*								R_Date Cooley AA17695	15.8 ± 0.14	*19 ± 0.2*	
BL18				*20 ± 0.4*							R_Date Port AA68976	15.6 ± 0.09	*18.9 ± 0.1*	
Scottish (?) readvance	T3JURB01	20.8 ± 2.4	*19.5 ± 0.7*								R_Date Port AA68975	15.7 ± 0.09	*19 ± 0.1*	
	T3JURB02	23.4 ± 2.8	*19.6 ± 0.6*								R_Date Port CAM-S105063	15.9 ± 0.05	*19.1 ± 0.1*	
	T3GUTT03	21.7 ± 2.6	*19.5 ± 0.7*								R_Date Port CAM-S105064	16.4 ± 0.06	*19.1 ± 0.4*	
BL19				*18.9 ± 1.1*						BL NE3				*18.7 ± 0.2*
Scottish (?) readvance	T3ALDO01	20.2 ± 3.5	*17.3 ± 1.1*							Cranfield Pt	R_Date Cranfield AA21819	16.0 ± 0.14	*18.4 ± 0.2*	
	T3ALDO02	27.9 ± 4.7	*								R_Date Cranfield AA21818	15.1 ± 0.13	*18.4 ± 0.2*	
B20				*15.5 ± 0.6*						BL NE4				*18.1 ± 0.2*
Galloway Hills	GB-02	12.0 ± 1.2	*		E BL10				*17.4 ± 0.8*	Linns-Rathcor	R_Date Rathcor AA56701	14.7 ± 0.13	*17.8 ± 0.1*	
	GB-03	14.8 ± 1.2	*15.1 ± 0.5*		Cumbria (Duddon - Shap)	C_Date Dudd01	16.5 ± 0.9	*16.8 ± 0.7*			R_Date Linns AA56700	14.6 ± 0.07	*17.7 ± 0.1*	
	GB-04	15.1 ± 0.9	*15.1 ± 0.5*			C_Date Dudd02	16.6 ± 0.9	*16.8 ± 0.7*		BL NI5 Killard Adv				*17.4 ± 0.3*
	GB-06	14.7 ± 1.4	*15.1 ± 0.5*			C_Date Dudd05	17.0 ± 0.9	*16.8 ± 0.7*		Killard Point	R_Date	13.8 ± 0.12	*16.8 ± 0.2*	

(*Continued*)

© 2021 The Authors *Journal of Quaternary Science* Published by John Wiley & Sons, Ltd.

10991417, 2021, 5, Downloaded from https://onlinelibrary.wiley.com/doi/10.1002/jqs.3313 by Ogs Trieste Istituto Nazionale, Wiley Online Library on [24/11/2023]. See the Terms and Conditions (https://onlinelibrary.wiley.com/terms-and-conditions) on Wiley Online Library for rules of use; OA articles are governed by the applicable Creative Commons License

Table 3. (*Continued*)

Irish Sea Ice Stream					Irish Sea Glacier					Retreat from N Irish Sea Basin				
Model structure	Age information	Unmodelled age	*Modelled age*	*Boundary age*	Model structure	Age information	Unmodelled age	*Modelled age*	*Boundary age*	Model structure	Age information	Unmodelled age	*Modelled age*	*Boundary age*
	GT-01	15.1 ± 0.9	*15.1 ± 0.5*			C_Date Dudd06	15.9 ± 0.9	*16.7 ± 0.7*			Killard Point2 R_Date Killard Point1	14.0 ± 0.11	*17 ± 0.2*	
	GT-2.1	15.5 ± 0.8	*15.2 ± 0.4*			C_Date Shap2	17.5 ± 1.0	*16.9 ± 0.7*		BL NI6 Killard Ret. Rough Isl.				*16.5 ± 0-.2*
	GT-2.2	15.3 ± 0.8	*15.2 ± 0.4*			C_Date Shap3	18.6 ± 0.9	*			R_Date Rough AA21822	12.7 ± 0.1	*15.3 ± 0.4*	
	GT-03	14.0 ± 0.7	*15 ± 0.5*			C_Date Shap7	16.7 ± 1.0	*16.8 ± 0.7*			R_Date Rough AA68680	13.5 ± 0.07	*16.3 ± 0.1*	
BL21				*14.8 ± 0.5*	E BL11				*16.2 ± 0.8*	BL NI Deglaciation				*15 ± 0.8*

© 2021 The Authors *Journal of Quaternary Science* Published by John Wiley & Sons, Ltd.

10991417, 2021, 5, Downloaded from https://onlinelibrary.wiley.com/doi/10.1002/jqs.3313 by Ogs Trieste Istituto Nazionale, Wiley Online Library on [24/11/2023]. See the Terms and Conditions (https://onlinelibrary.wiley.com/terms-and-conditions) on Wiley Online Library for rules of use; OA articles are governed by the applicable Creative Commons License

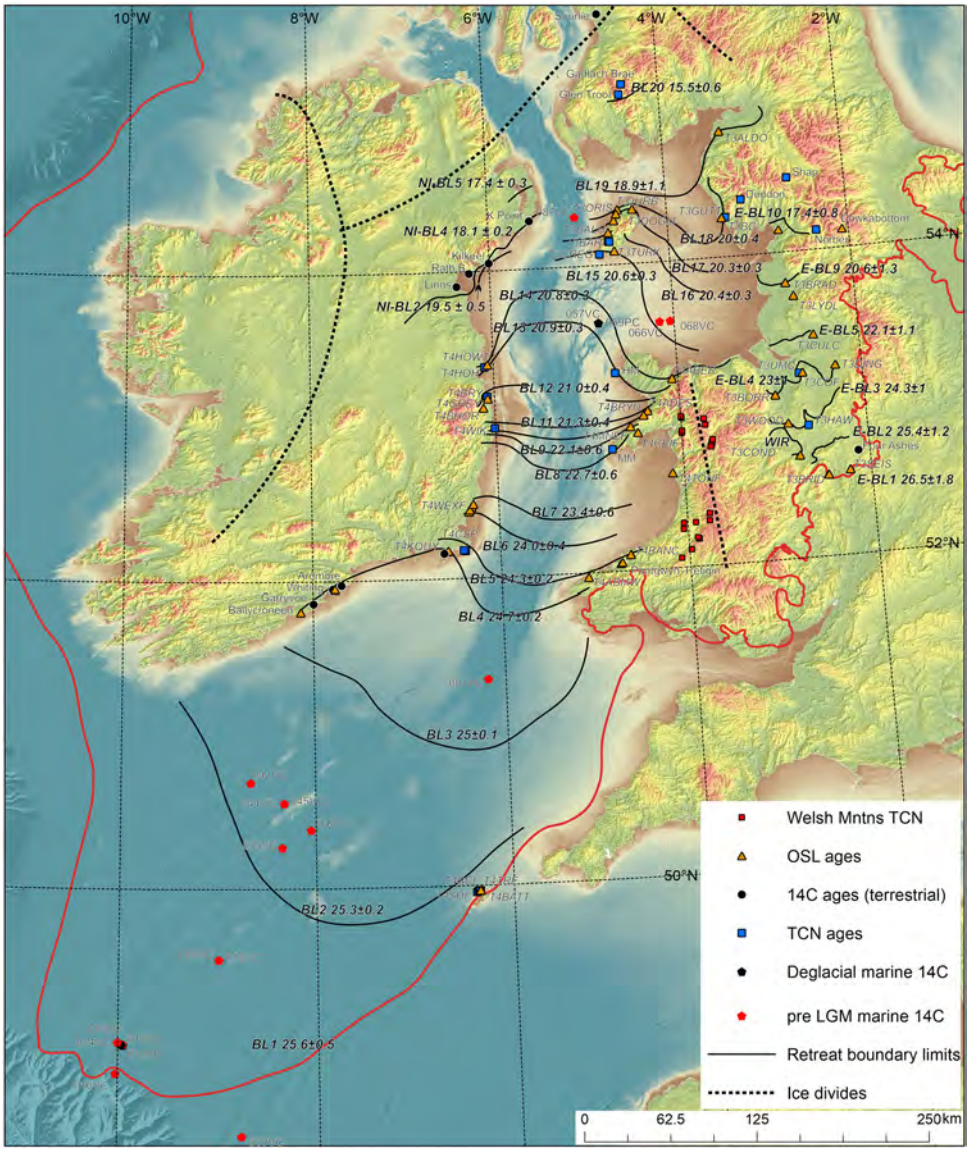

Figure 7. Chronology for the major retreat limits calculated in the Bayesian age modelling for the wider Irish Sea sector plotted over topographic and bathymetric data [the CGIAR-CSI SRTM (Version 4) 30-m-resolution (http://srtm.csi.cgiar.org/srtmdata/)] and EMODnet data (https://www.emodnet-bathymetry.eu/). The locations sampled for geochronology (^{14}C, TCN and OSL) are identified. The retreat limits show the boundary ages ±1σ for ISIS, retreat into the northeast of Ireland (Chiverrell *et al.*, 2018) and the ISG (English Midlands) (Chiverrell *et al.*, 2020). The ice divides shown represent ice maximum positions after which their position was dynamic; these are based on Clark *et al.* (2012) apart from the divide in the Galloway Hills based on Finlayson *et al.* (2010). [Color figure can be viewed at wileyonlinelibrary.com].

Sea interpreted to have been subject to readvance (Fig. 1). Whether this was a major readvance, or merely slight adjustments to the grounded margin during overall retreat, is uncertain. It is notable that there is a peak of Celtic Sea sourced IRD in the Goban Spur at 26 ka before a larger peak coincident with Heinrich event 2, and two smaller peaks afterwards (Haapaniemi *et al.*, 2010; Fig. 8). It is not yet clear whether the spread of ^{14}C ages, or the interpretation of readvance, relate to these temporally separated IRD peaks.

Lockhart *et al.* (2018) have generated a seismic-stratigraphic synthesis of the sub-bottom acoustic profile and core data collected during the *James Cook* (JC106) cruise. This indicates that the glacigenic facies of the Celtic Sea form part of the upper Little Sole Formation (cf. Pantin and Evans, 1984) and that the northwestern series of linear sediment megaridges of the Celtic Sea represent tidal bedforms anchored on an eroded subglacial landsystem. A clear distinction in morphology is apparent between the 'western' ridges and those in the southeast which Lockhart *et al.* (2018) attribute to the influence of this subglacial basement on subsequent ridge evolution. The implication of this is that the western ridges are coincident with the limit of the ISIS advance, whereas the eastern ridges lie outside this ice advance. This interpretation is supported by a clear morphological distinction between the ridges in the two sectors, with the western ridges being larger/longer and orientated NE–SW contrasting with smaller/shorter eastern ridges orientated NNE–SSW. This distribution is consistent with the boundary between glacitectonized and undeformed glacimarine sequences (Fig. 1).

There are no marine geological or geophysical data available currently to resolve the ISIS eastern flank limit or how the ISIS advance relates to the earlier ice advance postulated to have overridden Lundy in the outer Bristol Channel (Fig. 1; cf. Rolfe *et al.*, 2012) although the nature of any direct evidence of glaciation and associated timings in the outer Bristol Channel remain equivocal (Carr *et al.*, 2017; Gibbard *et al.*, 2017; Hiemstra *et al.*, 2019). However, the distribution of glacigenic sediments and landforms on Scilly (Scourse, 1991; Hiemstra *et al.*, 2006; Smedley *et al.*, 2017a) is difficult to explain without a major portion of the ISIS east flank

© 2021 The Authors *Journal of Quaternary Science* Published by John Wiley & Sons, Ltd.

10991417, 2021, 5, Downloaded from https://onlinelibrary.wiley.com/doi/10.1002/jqs.3313 by Ogs Trieste Istituto Nazionale, Wiley Online Library on [24/11/2023]. See the Terms and Conditions (https://onlinelibrary.wiley.com/terms-and-conditions) on Wiley Online Library for rules of use; OA articles are governed by the applicable Creative Commons License

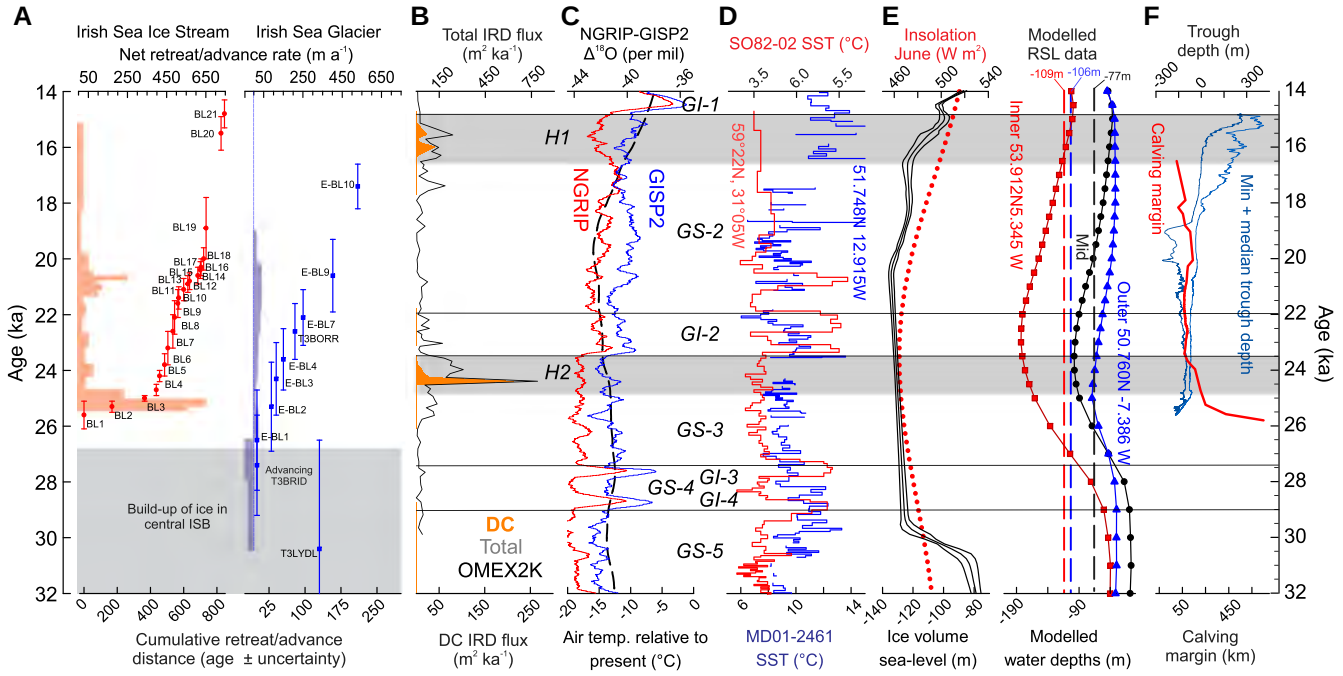

Figure 8. (A) Boundary ages (circle ±1σ whisker plots) from both the ISIS and ISG Bayesian models against the respective net axial distance (bottom axis); also plotted are net integrated axial advance/retreat rates in m a^{-1} (solid bars, top axis) calculated from the Bayesian models. (B) Total (outline) and detrital carbonate (orange) ice-rafted debris (IRD) flux records from the OMEX 2 K core (49°5′N, 13°26′W) (Haapaniemi *et al.*, 2010). Heinrich Events H2 and H1 are highlighted (Bond *et al.*, 1992). (C) $\delta^{18}O$ concentrations, Greenland Stadials (GS) and Interstadials (GI) from the GISP2 and NGRIP Greenland ice cores (Rasmussen *et al.*, 2014), and modelled surface-air temperatures (black line) relative to present for land masses north of ~45°N (Bintanja *et al.*, 2005). (D) Sea surface temperature (SST) records determined for the North Atlantic using SST (°C) calculated using planktonic foraminifera for core SO82-02 at 59°N, 31°W (red line) (Van Kreveld *et al.*, 2000; Rasmussen *et al.*, 2016) plotted using the Waelbroeck *et al.* (2019) age model and the MD01-2461 site from the Porcupine Seabight at 51.7°N, 12.9°W (blue line) (Peck *et al.*, 2006; Peck *et al.*, 2007). (E) Ice volume equivalent sea level including uncertainties (black/solid) (Lambeck *et al.*, 2014) plotted alongside summer insolation (red/pecked) for 60°N (Berger and Loutre, 1991), and modelled relative sea level water depths for the inner, mid- and outer ISIS derived from a glacio-isostatic adjustment model (Bradley *et al.*, 2011) updated to include the latest BRITICE-CHRONO ice sheet reconstruction and accounting for global ice sheet variations. Palaeo-water depths reproduced here are calculated by subtracting the predicted relative sea level from the present-day bathymetry. (F) Calving front width, and the minimum and median ice front elevations estimated from the NEXTMap elevation and EMODnet bathymetry (www.emodnet-hydrography.eu/) datasets for the ISIS plotted against the modelled boundary age chronology (Figs. 6 and 7). [Color figure can be viewed at wileyonlinelibrary.com].

overriding at least the western part of the Lundy Platform (Lockhart, 2019).

The youngest ^{14}C ages derived from shells reworked into Irish Sea Till along the south coast of Ireland (Ó Cofaigh and Evans, 2001a,b, 2007) post-date the shelf break maximum of *25.6 ± 0.5 ka* (BL1). In the Bayesian model they are included as a retreat stage cluster of ages, suggesting that they represent retreat-stage diamicts deposited during oscillatory retreat of the ISIS margins onshore across south and southeast Ireland.

Furze *et al.*'s (2014) interpretation of possible glacilacustrine deglaciation in the Celtic Deep supports early glacial isostatic adjustment (GIA) simulations of a landbridge between Britain and Ireland during deglaciation (Lambeck, 1995). Tóth *et al.* (2020) imply from geomorphological and seismostratigraphic evidence onshore and offshore the Irish southeast coast that a regional palaeolake developed following ice recession of the ISIS and they reconstruct a southerly advance of Irish Ice Sheet ice going at least 15 km offshore onto the shelf across County Waterford. No micropalaeontology has yet been undertaken on the JC106 piston cores so it has not been possible to further test whether deglaciation was marine or lacustrine. However, the glacigenic mud sequences at the base of the two cores are undeformed, with high water content, and are very soft, indicating that they have not been subsequently overridden by ice. This suggests that the terminus just to the south of St George's Channel retreated without the readvance phases characteristic of the Celtic Sea; this supports the interpretation of faster retreat across the reverse slope of the Celtic Deep (Small *et al.*, 2018).

West Wales and the central Irish Sea

The geochronology collected for southwest Wales (Pembrokeshire) and from the southern coast of Ireland together constrain the pullback of ice to the pinning point between southeast Ireland and southwest Wales after the advance to maximum limits (Fig. 7). OSL ages obtained for proglacial sediments on the Cork and Waterford coasts of southern Ireland have constrained the pull-back of ice margins from the coast to around 24.4 ± 1.8, 24.2 ± 2.3 (Whiting Bay) and 23.8 ± 2.1 ka (Ballycroneen Strand) (Ó Cofaigh *et al.*, 2012). Glasser *et al.* (2018) presented pairs of OSL ages from outwash deposits in Pembrokeshire (southwest Wales) exposed in the Pantgwyn and Trefigin Quarries. Those single grain OSL measurements targeted poorly sorted gravel and coarse to fine sand attributed to deposition by southerly flowing braided rivers at 29.1 ± 4.2, 26.2 ± 2.0 (both Pantgwyn), 28.1 ± 1.9 and 22.8 ± 3.2 ka (Trefigin). From this and considering that the ages overlapped with admittedly wide uncertainties, Glasser *et al.* (2018) calculated weighted mean ages both centred on ~26.7 ka for sediments attributed to a post-maximum ice extent stage of the ISIS retreat sequence. This is problematic, as they pre-date the timing for maximum positions obtained for the south Celtic Sea (Praeg *et al.*, 2015; Smedley *et al.*, 2017a; Scourse *et al.*, 2019).

As part of BRITICE-CHRONO further OSL ages were determined from Kilmore Quay (25.7 ± 4.7 and 26.2 ± 2.2 ka) and TCN ages from Carnsore Point (27.8 ± 1.5 and 24.0 ± 1.3 ka), both in southeast Ireland (Small *et al.*, 2018).

© 2021 The Authors *Journal of Quaternary Science* Published by John Wiley & Sons, Ltd.

10991417, 2021, 5, Downloaded from https://onlinelibrary.wiley.com/doi/10.1002/jqs.3313 by Ogs Trieste Istituto Nazionale, Wiley Online Library on [24/11/2023]. See the Terms and Conditions (https://onlinelibrary.wiley.com/terms-and-conditions) on Wiley Online Library for rules of use; OA articles are governed by the applicable Creative Commons License

Here, the OSL age determined for sample T4ABMW01 at Abermawr (Fig. 5a; 25.2 ± 5.0 ka) is consistent with the chronology from Pembroke and southern Ireland. The OSL ages from Banc-y-Warren, T4BANC01 (Fig. 5b; 22.1 ± 3.6 ka) and T4BANC02 (Fig. 5c; 39.6 ± 5.7 ka), are in stratigraphical order within the sedimentary sequence. It is possible that the large difference between the two ages is due to the minimum dose population being characterized better for sample T4BANC01 (Fig. 5b) than for sample T4BANC02 (Fig. 5c). In the Bayesian model (Fig. 6) all the ages mentioned have been incorporated as a single Phase containing the Waterford–Kilmore–Carnsore–Pembroke retreat stage geochronology. This model structure produces a good fit, achieved by handling the older ages from Banc-y-Warren, Pantgwyn, Trefigin (all OSL) and Carnsore Point (TCN) as outliers. The boundary ages produced by the Bayesian model suggest that ice had retreated from this north Pembroke – south Wexford – Waterford alignment between 24.3 ± 0.2 ka (BL5) and 24.0 ± 0.4 ka (BL6; Fig. 7).

The timing of ice margin retreat north from St George's Channel, interpreted based on the Bayesian analysis of the BRITICE-CHRONO data, suggests significant deglaciation by ~23.3 ka. The OSL age determined for sample T4TONF01 (17.2 ± 1.6 ka) is younger than the adjacent OSL chronology from the Llŷn Peninsula (Smedley *et al.*, 2017b), and even the southern portion of the Isle of Man (Chiverrell *et al.*, 2018). Given the stratigraphical position of the OSL sample at Tonfanau, this age may instead date late-stage reworking of the deposit either as a subaerial sandur sourced from Welsh ice or periglacial fluvial remobilization (Patton and Hambrey, 2009). In either case, the Tonfanau OSL age provides limited constraint on passage northwards of Irish Sea ice margins and was excluded from the Bayesian model on the grounds of context.

The pace of ice margin retreat slowed as the ice stream narrows between SE Ireland and SW Wales, and there was probably a minor readvance and stabilization of the ice marginal position between *24.7 ± 0.2 ka* (BL4) and *24.2 ± 0.2 ka* (BL5). The pace of net axial ice margin retreat remains slower, 20–40 m a^{-1}, moving northwards from BL5 (*24.2 ± 0.2 ka*) through the Llŷn Peninsula to Wicklow alignment by *22.1 ± 0.6 ka* (BL9), overlapping with a narrower constriction of the palaeo-ice stream (Fig. 7). The northern end of the Wicklow Trough may mark this transition from rapid to slow retreat (Coughlan *et al.*, 2020). There is evidence for a slight acceleration of retreat through the wider portion of Cardigan Bay, north of the extensive Screen Hills moraine complex in County Wexford (BL7) (Thomas and Summers, 1983, 1984; Small *et al.*, 2018). Across the Wicklow – Llŷn Peninsula configurations of the ice margin (BL8 to BL12; Fig. 7), between *22.6 ± 0.6* and *21.4 ± 0.4* ka, the pace of net axial margin retreat was slow initially (~25 m a^{-1}) and with an oscillatory ice front (Thomas and Chiverrell, 2007), but then accelerated (~125 m a^{-1}) as the ice front widened and pulled back from a reverse bed slope into the deeper water of the northern St George's Channel (Smedley *et al.*, 2017a).

Northern Irish Sea Basin

The temporal correlations of EBL5 with the ISIS margins at a Wicklow – Llŷn Peninsula position provides a mechanism for ponding the extensive proglacial lakes that developed in the Manchester embayment, the rivers Weaver (Glacial Lakes Delamere and Congleton) and Dee (Glacial Lake Bangor) basins (Crofts, 2005; Chiverrell *et al.*, 2021). In addition, this configuration of the ice margins would have created circumstances conducive for ice-dammed lakes in northeast Wales (Peake, 1961; Thomas, 2005). Retreat of ice margins through the central Irish Sea displays marked asymmetry with more rapid retreat (100–250 m a^{-1}) across the western deeper waters (Fig. 7). With >130 m typical water depths at present and extending to join the North Channel between northeast Ireland and southwest Scotland, ice margins reached the coastline of northeast Ireland between *21 ± 0.4 ka* (NE-BL1) and *19.5 ± 0.5 ka* (NE-BL2). In the east the ISIS margins retreated across the shallower (>65 m) eastern Irish Sea and across the Isle of Man *20.6 ± 0.3 ka* (BL15) to *20 ± 0.4* (BL18) ka. The sea floor geomorphology between the Isle of Man and Wales reflects these changing glacial dynamics, with ribbed moraine and latterly drumlinized subglacial bedforms evidencing a more southwest to westerly flow direction and renewed ice streaming conditioned by the topography and increasing proglacial space in the western Irish Sea (Van Landeghem *et al.*, 2009; Van Landeghem and Chiverrell, 2020).

Readvances of the ice margins characterize the glacial dynamics during the step back across the northern ISB and into northeast Ireland (Fig. 7). These include the Scottish Readvance (Trotter *et al.*, 1937) constrained in the Bayesian model to between *20 ± 0.4* and *18.9 ± 1.1* ka (BL18-19), but predating advance limits (possibly linked with H1) in the north of Ireland. Geomorphological evidence for >1–2-km-scale readvances of the ice margin is unequivocal on the Isle of Man and western Cumbria (Huddart, 1977; Thomas *et al.*, 2004; Livingstone *et al.*, 2010; Chiverrell *et al.*, 2018). Readvances of the ice margins in northeast Ireland occurred *18.7 ± 0.2 ka* (NI-BL3) and at Killard Point *17.4 ± 0.3* to *16.5 ± 0.2* ka overlapping with Heinrich event 1 (McCabe, 2008; Ballantyne and Ó Cofaigh, 2017; Chiverrell *et al.*, 2018), but there is a lack of a dated limit position equivalent to Killard Point in the northeast Irish Sea; it may be situated in the Solway Firth. Ultimately, the Bayesian model shows similar ages for retreat and deglaciation of mountain regions in southwest Scotland and the English Lake District ~16–15 ka (cf. Ballantyne *et al.*, 2013; Wilson *et al.*, 2018).

Controls on ice advance, maximum extent and deglaciation

The available terrestrial and shallow marine geochronological evidence indicates that significant ice sheet growth in this sector of the BIIS initiated before 26 ka and probably around 30 ka (Fig. 8) although the deep ocean IRD record indicates clearly BIIS calving margins in Marine Isotope Stage (MIS) 3 and initiation during the MIS5/4 transition (Scourse *et al.*, 2009). The IRD record indicates that initial ice sheet growth and readvance dynamics in MIS3 appear tightly coupled to millennial-scale external climate forcing (Scourse *et al.*, 2009). Ice in the ISB had expanded as far south as central Lancashire by ~30–29 ka (Fig. 8) (Chiverrell *et al.*, 2020). The expansion to maximum extent of the ISIS revealed here is early in the global Last Glacial Maximum (LGM) at *25.6 ± 0.5 ka* (Clark *et al.*, 2009). The ISG reached maximum limits slightly earlier than the maximum extent of the ISIS, at *26.4 ± 1.1 ka*, and with a slower net axial advance rate of ~35 m a^{-1} (Fig. 8). In 4000 years the marine terminating ISIS had accomplished 565 km of axial ice margin retreat (BL1 to BL10), which contrasts markedly with the terrestrial-terminating ISG reaching eBL5 by *22.1 ± 1.1 ka*, some 115 km at only 26 m a^{-1} (Figs. 7 and 8).

The data are consistent with the build-up of ice within the ISB ~30 ka through to 26 ka and then rapid advance across the shallow southern Celtic Sea soon after; whether this advance was associated with ice streaming or not is unclear, but rapid splaying of the ice front into the Celtic Sea, more than 300 km south of the constriction of St George's Channel suggests rapid advance as a piedmont lobe across the full width of the ice

© 2021 The Authors *Journal of Quaternary Science* Published by John Wiley & Sons, Ltd.

10991417, 2021, 5, Downloaded from https://onlinelibrary.wiley.com/doi/10.1002/jqs.3313 by Ogs Trieste Istituto Nazionale, Wiley Online Library on [24/11/2023]. See the Terms and Conditions (https://onlinelibrary.wiley.com/terms-and-conditions) on Wiley Online Library for rules of use; OA articles are governed by the applicable Creative Commons License

front. Some support for ice streaming during this advance is provided by the extensive mega-scale glacial lineations north of Anglesey where these bedforms are >60 km in length and aligned NNE–SSW parallel to ice flow towards the Celtic Sea (Van Landeghem and Chiverrell, 2020). This advance can be conceived of as a response and temporary over-extension of the ice front preceded and conditioned by significant ice accumulation behind the St George's Channel topographic barrier which steepened the ice surface profile to beyond its yield stress. Once released, the ISIS is interpreted to have captured ice that formerly fed into Cheshire–Shropshire from the ISG from accumulation in the hinterland of the northern ISB and redirected this ice into the main axis of the Irish Sea. This ice piracy starved the terrestrial ISG of ice and initiated slow and early deglaciation, evidenced by the dead ice land system ubiquitous in the Cheshire–Shropshire lowlands (Chiverrell *et al.*, 2020). Deglaciation of the ISIS from its maximum extent at the Celtic shelf break followed soon afterwards because of ice starvation following the over-extension event accentuated along a very wide marine margin.

The plausibility of our reconstructed behaviour of ice stream over-extension and ice catchment piracy could be usefully tested by ice sheet modelling experiments. However, in the absence of this it is clear that the timing of this rapid deglaciation event must surely be a function primarily of internal ice dynamic effects as it clearly precedes the warming of Greenland interstadial 2 that followed Heinrich Event 2 and it is not associated with any significant increase in relative sea level (Fig. 8). Thereafter, the sequence of deglaciation of the ISIS and readvance dynamics of the Ice Stream were strongly conditioned by topographic factors, notably trough geometry, rather than simply by external climatic or sea level controls (Fig. 8; Smedley *et al.*, 2017a; Small *et al.*, 2018). External climatic controls, including marine and atmospheric temperature regimes, and precipitation, seem to have played a significant role in early ice growth in this sector of the BIIS. Thereafter, at maximum extent and during deglaciation, ice dynamics and topographic controls exerted a stronger role (Fig. 8).

Conclusions

The Irish Sea sector of the former BIIS differs from all other sectors in that it was a compound (bifurcating) system with two outlets, one a marine-terminating ice stream flowing southwards through the ISB into the Celtic Sea, the ISIS, and a non-streaming terrestrial terminus flowing southwards through Cheshire–Shropshire lowlands into the English Midlands, denoted the ISG. This contrast constitutes a natural laboratory for identifying major drivers of deglaciation since marine forcing was absent in the Cheshire–Shropshire sector until late in deglaciation. The timing and readvance dynamics of both the ISIS and the ISG have been reconstructed via a Bayesian analysis of the geochronological data from both on- and offshore sequences.

The regional chronology (Fig. 8) shows that ice in the Irish Sea sector built-up and expanded substantially from 30 ka through to ~26 ka (Chiverrell *et al.*, 2020). The ISIS extended as far as the continental shelf break to the SW of Britain and Ireland at *25.6 ± 0.5 ka*; independently dated IRD is registered from the ISIS in adjacent deep-sea cores synchronous with this advance. The ISIS then retreated rapidly northwards through the Celtic Sea, with evidence for readvance phases reaching St George's Channel by 24.3 ka and the Llŷn Peninsula by 23.9 ka. The complex readvance sequences identified on the Llŷn Peninsula (24–20 ka) and in eastern Ireland have now been tightly constrained to register centennial-scale oscillations of the ice front driven by internal ice dynamics over topographic pinning points and constrictions of the ice-stream. The ISG in the Cheshire–Shropshire lowlands displayed differing dynamics with little evidence of streaming but reached a slightly earlier maximum at *26.4 ± 1.1 ka*, with confining topography and the interaction with ice-dammed lakes contributing to regulate the terrestrial retreat dynamics, eventually pulling back offshore by ~21 ka. Retreat northwards into the northern Irish Sea then accelerated, evacuating the deeper waters of the western Irish Sea first, developing pronounced ice margins across the northern Isle of Man by 19.1 ka. The final retreat phase, with ice margins pulling back onto terrestrial settings in the north of Ireland and SW Scotland around 17 ka, was ultimately deglaciation accomplished in a fully marine context as evidenced by the preservation on the seabed of subglacial landforms and by increasing influence of local ice sources with flow realignment during drawn-down and retreat.

The timing and patterns of retreat of the ISIS and ISG revealed by this analysis suggest a 'plugging' of ISIS behind the St George's Channel topographic barrier steepening the ice surface profile, which once released produced a rapid over-extension into the Celtic Sea. This initiated piracy of the ISG through the capturing of ice accumulation sources in the northern ISB ultimately leading to slow deglaciation characterized by a dead ice landsystem. Initial deglaciation of the ISIS from the shelf-break is therefore attributed to ice starvation following its temporary over-extension, and its overall retreat behaviour was largely marine in character and strongly modulated by topographic controls.

Supporting information

Additional supporting information can be found in the online version of this article.

Acknowledgements. This research was supported by a Natural Environment Research Council consortium grant (BRITICE-CHRONO NE/J008672/1). Thanks are due to Sally Morgan and Elke Hanenkamp (University of Leicester) for acquisition and processing of multi-sensor core-logger data. The work was supported by the NERC Radiocarbon Facility (allocations 1530.0311, 1577.0911 and 1606.0312) and the NERC Cosmogenic Isotope Analysis Facility. We thank the staff at the SUERC AMS Laboratory, East Kilbride, for carbon isotope measurements, and the master and crew of the RRS *James Cook*, the BGS Marine Operations Team (vibrocorer) and the NOC/NMEP (piston corer). Daniel Praeg's participation has been in part supported by the Italian PNRA project IPY GLAMAR (grant no. 2009/A2.15). We thank two anonymous reviewers for their helpful and constructive comments.

Data Availability Statement

The data that support the findings of this study are included in the text and Supporting Information, or previously published sources as cited. All relevant data will also be made available in the forthcoming BRITICE-CHRONO online data repository, or upon reasonable request from the lead author.

Abbreviations. BIIS, British–Irish Ice Sheet; BL, Boundary Limit; FMM, finite mixture model; GIA, glacial isostatic adjustment; GS, Greenland stadial; ICP-MS, inductively coupled plasma mass spectrometry; IRD, ice-rafted detritus; ISB, Irish Sea Basin; ISG, Irish Sea Glacier; ISIS, Irish Sea Ice Stream; LGM, Last Glacial Maximum; MAM, minimum age model; MCMC, Markov chain Monte Carlo; MIS, Marine Isotope Stage; OSL, optically stimulated luminescence; TCN, terrestrial cosmogenic nuclide.

© 2021 The Authors *Journal of Quaternary Science* Published by John Wiley & Sons, Ltd.

10991417, 2021, 5, Downloaded from https://onlinelibrary.wiley.com/doi/10.1002/jqs.3313 by Ogs Trieste Istituto Nazionale, Wiley Online Library on [24/11/2023]. See the Terms and Conditions (https://onlinelibrary.wiley.com/terms-and-conditions) on Wiley Online Library for rules of use; OA articles are governed by the applicable Creative Commons License

References

Allen JRL. 1982. Late Pleistocene (Devensian) glaciofluvial outwash at Banc-Y-Warren, near Cardigan (West Wales). *Geological Journal* **17**: 31–47.

Alley RB, Blankenship DD, Bentley CR *et al*. 1986. Deformation of till beneath ice stream B, West Antarctica. *Nature* **322**: 57–59. https://doi.org/10.1038/322057a0

Austin WEN, McCarroll D. 1992. Foraminifera from the Irish Sea glacigenic deposits at Aberdaron, western Lleyn, North Wales: palaeoenvironmental implications. *Journal of Quaternary Science* **7**: 311–317. https://doi.org/10.1002/jqs.3390070406

Austin WEN, Scourse JD. 1997. Evolution of seasonal stratification in the Celtic Sea during the Holocene. *Journal of the Geological Society* **154**: 249–256. https://doi.org/10.1144/gsjgs.154.2.0249

Ballantyne CK, Ó Cofaigh C 2017. The last Irish Ice Sheet: extent and chronology. In Coxon P, McCarron S, Mitchell F (eds). Advances in Irish Quaternary Studies. Springer: Berlin: 101–149.

Ballantyne CK, Rinterknecht V, Gheorghiu DM. 2013. Deglaciation chronology of the Galloway Hills Ice Centre, southwest Scotland. *Journal of Quaternary Science* **28**: 412–420. https://doi.org/10.1002/jqs.2635

Ballantyne CK, Small D. 2019. The Last Scottish Ice Sheet. *Earth and Environmental Science Transactions of the Royal Society of Edinburgh* **110**: 93–131. https://doi.org/10.1017/S1755691018000038

Berger A, Loutre MF. 1991. Insolation values for the climate of the last 10 million years. *Quaternary Science Reviews* **10**: 297–317. https://doi.org/10.1016/0277-3791(91)90033-Q

Bintanja R, van de Wal RSW, Oerlemans J. 2005. Modelled atmospheric temperatures and global sea levels over the past million years. *Nature* **437**: 125–128. https://doi.org/10.1038/nature03975. [PubMed: 16136140].

Bond G, Heinrich H, Broecker W *et al*. 1992. Evidence for massive discharges of icebergs into the North Atlantic Ocean during the last glacial period. *Nature* **360**: 245–249. https://doi.org/10.1038/360245a0

Bøtter-Jensen L, Andersen CE, Duller GAT *et al*. 2003. Developments in radiation, stimulation and observation facilities in luminescence measurements. *Radiation Measurements* **37**: 535–541. https://doi.org/10.1016/S1350-4487(03)00020-9

Bowen DQ 1973. The Pleistocene succession of the Irish Sea. *Proceedings of the Geologists' Association* **84**: 249–IN2. https://doi.org/10.1016/S0016-7878(73)80034-3

Bradley SL, Milne GA, Shennan I *et al*. 2011. An improved glacial isostatic adjustment model for the British Isles. *Journal of Quaternary Science* **26**: 541–552. https://doi.org/10.1002/jqs.1481

Bradwell T, Small D, Fabel D *et al*. 2019. Pattern, style and timing of British–Irish Ice Sheet retreat: Shetland and northern North Sea sector. *Journal of Quaternary Science*. https://doi.org/10.1002/jqs.3163

Bronk Ramsey C. 2009a. Bayesian analysis of radiocarbon dates. *Radiocarbon* **51**: 337–360. https://doi.org/10.1017/S0033822200033865

Bronk Ramsey C. 2009b. Dealing with outliers and offsets in radiocarbon dating. *Radiocarbon* **51**: 1023–1045. https://doi.org/10.1017/S0033822200034093

Bronk Ramsey CB. 2008. Deposition models for chronological records. *Quaternary Science Reviews* **27**: 42–60. https://doi.org/10.1016/j.quascirev.2007.01.019

Bronk Ramsey CB, Lee S. 2013. Recent and planned developments of the program OxCal. *Radiocarbon* **55**: 720–730. https://doi.org/10.1017/S0033822200057878

Brown EJ, Rose J, Coope RG *et al*. 2007. An MIS 3 age organic deposit from Balglass Burn, central Scotland: palaeoenvironmental significance and implications for the timing of the onset of the LGM ice sheet in the vicinity of the British Isles. *Journal of Quaternary Science* **22**: 295–308. https://doi.org/10.1002/jqs.1028

Buck CE, Cavanagh WG, Litton CD. 1996. *Bayesian Approach to Interpreting Archaeological Data. Statistics in Practice*. Wiley: Chichester.

Carr SJ, Hiemstra JF, Owen G. 2017. Landscape evolution of Lundy Island: challenging the proposed MIS 3 glaciation of SW Britain. *Proceedings of the Geologists' Association* **128**: 722–741. https://doi.org/10.1016/j.pgeola.2017.06.005

Charlesworth JK. 1929. The south Wales end-moraine. *Quarterly Journal of the Geological Society* **85**: 335–358. https://doi.org/10.1144/GSL.JGS.1929.085.01-04.11

Chiverrell RC, Burke MJ, Thomas GSP. 2016. Morphological and sedimentary responses to ice mass interaction during the last deglaciation. *Journal of Quaternary Science* **31**: 265–280. https://doi.org/10.1002/jqs.2864

Chiverrell RC, Foster GC, Thomas GSP *et al*. 2009. Robust chronologies for landform development. *Earth Surface Processes and Landforms* **34**: 319–328. https://doi.org/10.1002/esp.1720

Chiverrell RC, Smedley RK, Small D *et al*. 2018. Ice margin oscillations during deglaciation of the northern Irish Sea Basin. *Journal of Quaternary Science* **33**: 739–762. https://doi.org/10.1002/jqs.3057

Chiverrell RC, Thomas GSP, Burke M *et al*. 2021. The evolution of the terrestrial-terminating Irish Sea glacier during the last glaciation. *Journal of Quaternary Science*. https://doi.org/10.1002/jqs.3229

Chiverrell RC, Thrasher IM, Thomas GSP *et al*. 2013. Bayesian modelling the retreat of the Irish Sea Ice Stream. *Journal of Quaternary Science* **28**: 200–209. https://doi.org/10.1002/jqs.2616

Clark CD, Hughes ALC, Greenwood SL *et al*. 2012. Pattern and timing of retreat of the last British–Irish Ice Sheet. *Quaternary Science Reviews* **44**: 112–146. https://doi.org/10.1016/j.quascirev.2010.07.019

Clark PU, Dyke AS, Shakun JD *et al*. 2009. The last glacial maximum. *Science* **325**: 710–714.

Coughlan M, Tóth Z, Van Landeghem KJJ *et al*. 2020. Formational history of the Wicklow Trough: a marine-transgressed tunnel valley revealing ice flow velocity and retreat rates for the largest ice stream draining the late-Devensian British–Irish Ice Sheet. *Journal of Quaternary Science* **35**: 907–919. https://doi.org/10.1002/jqs.3234

Crofts RG. 2005. *Quaternary of the Rossendale Forest and Greater Manchester: Field Guide*. Quaternary Research Association: London.

Duller GAT. 2008. Single-grain optical dating of Quaternary sediments: why aliquot size matters in luminescence dating. *Boreas* **37**: 589–612. https://doi.org/10.1111/j.1502-3885.2008.00051.x

Durcan JA, King GE, Duller GAT. 2015. DRAC: Dose Rate and Age Calculator for trapped charge dating. *Quaternary Geochronology* **28**: 54–61. https://doi.org/10.1016/j.quageo.2015.03.012

Finlayson A, Fabel D, Bradwell T *et al*. 2014. Growth and decay of a marine terminating sector of the last British–Irish Ice Sheet: a geomorphological reconstruction. *Quaternary Science Reviews* **83**: 28–45. https://doi.org/10.1016/j.quascirev.2013.10.009

Finlayson A, Merritt J, Browne M *et al*. 2010. Ice sheet advance, dynamics, and decay configurations: evidence from west central Scotland. *Quaternary Science Reviews* **29**: 969–988. https://doi.org/10.1016/j.quascirev.2009.12.016

Furze MFA, Scourse JD, Pieńkowski AJ *et al*. 2014. Deglacial to postglacial palaeoenvironments of the Celtic Sea: lacustrine conditions versus a continuous marine sequence. *Boreas* **43**: 149–174. https://doi.org/10.1111/bor.12028

Galbraith RF, Laslett GM. 1993. Statistical models for mixed fission track ages. *Nuclear Tracks and Radiation Measurements* **21**: 459–470. https://doi.org/10.1016/1359-0189(93)90185-C

Galbraith RF, Roberts RG, Laslett GM *et al*. 1999. Optical dating of single and multiple grains of quartz from Jinmium rock shelter, northern Australia: Part 1, experimental design and statistical models. *Archaeometry* **41**: 339–364. https://doi.org/10.1111/j.1475-4754.1999.tb00987.x

Gibbard PL, Hughes PD, Rolfe CJ. 2017. New insights into the Quaternary evolution of the Bristol Channel, UK. *Journal of Quaternary Science* **32**: 564–578. https://doi.org/10.1002/jqs.2951

Glasser NF, Davies JR, Hambrey MJ *et al*. 2018. Late Devensian deglaciation of south-west Wales from luminescence and cosmogenic isotope dating. *Journal of Quaternary Science* **33**: 804–818. https://doi.org/10.1002/jqs.3061

Guérin G, Mercier N, Adamiec G. 2011. Dose-rate conversion factors: update. *Ancient TL* **29**: 5–8.

Guérin G, Mercier N, Nathan R *et al*. 2012. On the use of the infinite matrix assumption and associated concepts: A critical review. *Radiation Measurements* **47**: 778–785. https://doi.org/10.1016/j.radmeas.2012.04.004

Haapaniemi AI, Scourse JD, Peck VL *et al*. 2010. Source, timing, frequency and flux of ice-rafted detritus to the northeast Atlantic

© 2021 The Authors *Journal of Quaternary Science* Published by John Wiley & Sons, Ltd.

10991417, 2021, 5, Downloaded from https://onlinelibrary.wiley.com/doi/10.1002/jqs.3313 by Ogs Trieste Istituto Nazionale, Wiley Online Library on [24/11/2023]. See the Terms and Conditions (https://onlinelibrary.wiley.com/terms-and-conditions) on Wiley Online Library for rules of use; OA articles are governed by the applicable Creative Commons License

margin, 30–12 ka: testing the Heinrich precursor hypothesis. *Boreas* **39** no. https://doi.org/10.1111/j.1502-3885.2010.00141.x

Hambrey MJ, Davies JR, Glasser NF *et al*. 2001. Devensian glacigenic sedimentation and landscape evolution in the Cardigan area of southwest Wales. *Journal of Quaternary Science* **16**: 455–482. https://doi.org/10.1002/jqs.639

Helm DG, Roberts B. 1975. A re-interpretation of the origin of sands and gravels around Banc-y-Warren, near Cardigan, West Wales. *Geological Journal* **10**: 131–146. https://doi.org/10.1002/gj.3350100203

Hiemstra JF, Evans DJA, Scourse JD *et al*. 2006. New evidence for a grounded Irish Sea glaciation of the Isles of Scilly, UK. *Quaternary Science Reviews* **25**: 299–309. https://doi.org/10.1016/j.quascirev.2005.01.013

Hiemstra JF, Shakesby RA, Owen G *et al*. 2019. Caldey ("Kald Ey" in Old Norse) was literally a 'cold island', but was it under Devensian ice? *Quaternary Newsletter* **148**: 21–31.

Huddart D. 1977. Field guide for excursion A4, X INQUA Congress. In Tooley, MJ (ed), *The Isle of Man, Lancashire Coast and Lake District*. Norwich: Geo Abstracts; 38–40.

Hughes PD, Glasser NF, Fink D. 2016. Rapid thinning of the Welsh Ice Cap at 20–19ka based on ^{10}Be ages. *Quaternary Research* **85**: 107–117. https://doi.org/10.1016/j.yqres.2015.11.003

Jenkins GTH, Duller GAT, Roberts HM *et al*. 2018. A new approach for luminescence dating glaciofluvial deposits – High precision optical dating of cobbles. *Quaternary Science Reviews* **192**: 263–273. https://doi.org/10.1016/j.quascirev.2018.05.036

Jones OT. 1965. The glacial and post-glacial history of the lower Teifi Valley. *Quarterly Journal of the Geological Society* **121**: 247–281. https://doi.org/10.1144/gsjgs.121.1.0247

Lambeck K. 1995. Late Devensian and Holocene shorelines of the British Isles and North Sea from models of glacio-hydro-isostatic rebound. *Journal of the Geological Society* **152**: 437–448. https://doi.org/10.1144/gsjgs.152.3.0437

Lambeck K, Rouby H, Purcell A *et al*. 2014. Sea level and global ice volumes from the Last Glacial Maximum to the Holocene. *Proceedings of the National Academy of Sciences of the United States of America* **111**: 15296–15303. https://doi.org/10.1073/pnas.1411762111. [PubMed: 25313072].

Lewis CA, Richards AE. 2005. *The Glaciations of Wales and Adjacent Areas*. Logaston Press: Eardisley.

Livingstone SJ, Evans DJA, O Cofaigh C. 2010. Re-advance of Scottish ice into the Solway Lowlands (Cumbria, UK) during the Main Late Devensian deglaciation. *Quaternary Science Reviews* **29**: 2544–2570.

Lockhart EA 2019. *Glacial sculpting and post-glacial drowning of the Celtic Sea* PhD Thesis, Bangor University.

Lockhart EA, Scourse JD, Praeg D *et al*. 2018. A stratigraphic investigation of the Celtic Sea megaridges based on seismic and core data from the Irish-UK sectors. *Quaternary Science Reviews* **198**: 156–170. https://doi.org/10.1016/j.quascirev.2018.08.029

McCabe AM. 2008. *Glacial Geology and Geomorphology: the Landscapes of Ireland*. Dunedin Academic Press: Edinburgh.

McCabe AM, Clark PU, Clark J *et al*. 2007. Radiocarbon constraints on readvances of the British–Irish Ice Sheet in the northern Irish Sea Basin during the last deglaciation. *Quaternary Science Reviews* **26**: 1204–1211. https://doi.org/10.1016/j.quascirev.2007.01.010

McCabe M, Knight J, McCarron S. 1998. Evidence for Heinrich event 1 in the British Isles. *Journal of Quaternary Science* **13**: 549–568. https://doi.org/10.1002/(SICI)1099-1417(1998110)13:6<549::AID-JQS394>3.0.CO;2-A

McCarroll D, Ballantyne CK. 2000. The last ice sheet in Snowdonia. *Journal of Quaternary Science* **15**: 765–778. https://doi.org/10.1002/1099-1417(200012)15:8<765::AID-JQS557>3.0.CO;2-P

McCarroll D, Rijsdijk KF. 2003. Deformation styles as a key for interpreting glacial depositional environments. *Journal of Quaternary Science* **18**: 473–489. https://doi.org/10.1002/jqs.780

McCarroll D, Stone JO, Ballantyne CK *et al*. 2010. Exposure-age constraints on the extent, timing and rate of retreat of the last Irish Sea ice stream. *Quaternary Science Reviews* **29**: 1844–1852. https://doi.org/10.1016/j.quascirev.2010.04.002

Mitchell GF. 1972. The Pleistocene history of the Irish Sea: second approximation. *Scientific Proceedings of the Royal Dublin Society* **4**: 181–199.

Mitchell GF, Orme AR. 1967. The Pleistocene deposits of the Isles of Scilly. *Quarterly Journal of the Geological Society* **123**: 59–92. https://doi.org/10.1144/gsjgs.123.1.0059

Morgan AV. 1973. The Pleistocene geology of the area North and west of Wolverhampton, Staffordshire, England. *Philosophical Transactions of the Royal Society of London* **265**: 233–297.

Murray AS, Wintle AG. 2000. Luminescence dating of quartz using an improved single-aliquot regenerative-dose protocol. *Radiation Measurements* **32**: 57–73. https://doi.org/10.1016/S1350-4487(99)00253-X

Ó Cofaigh C, Evans DJA. 2001a. Deforming bed conditions associated with a major ice stream of the last British ice sheet. *Geology* **29**: 795–798. https://doi.org/10.1130/0091-7613(2001)029<0795:DBCAWA>2.0.CO;2

Ó Cofaigh C, Evans DJA. 2001b. Sedimentary evidence for deforming bed conditions associated with a grounded Irish Sea glacier, southern Ireland. *Journal of Quaternary Science* **16**: 435–454. https://doi.org/10.1002/jqs.631

Ó Cofaigh C, Evans DJA. 2007. Radiocarbon constraints on the age of the maximum advance of the British–Irish Ice Sheet in the Celtic Sea. *Quaternary Science Reviews* **26**: 1197–1203. https://doi.org/10.1016/j.quascirev.2007.03.008

Ó Cofaigh C, Telfer MW, Bailey RM *et al*. 2012. Late Pleistocene chronostratigraphy and ice sheet limits, southern Ireland. *Quaternary Science Reviews* **44**: 160–179. https://doi.org/10.1016/j.quascirev.2010.01.011

Pantin HM, Evans CDR. 1984. The Quaternary history of the central and southwestern Celtic Sea. *Marine Geology* **57**: 259–293. https://doi.org/10.1016/0025-3227(84)90202-0

Patton H, Hambrey MJ. 2009. Ice-marginal sedimentation associated with the Late Devensian Welsh Ice Cap and the Irish Sea Ice Stream: Tonfanau, West Wales. *Proceedings of the Geologists' Association* **120**: 256–274. https://doi.org/10.1016/j.pgeola.2009.10.004

Patton H, Hubbard A, Bradwell T *et al*. 2013a. Rapid marine deglaciation: asynchronous retreat dynamics between the Irish Sea Ice Stream and terrestrial outlet glaciers. *Earth Surface Dynamics* **1**: 53–65. https://doi.org/10.5194/esurf-1-53-2013

Patton H, Hubbard A, Glasser NF *et al*. 2013b. The last Welsh Ice Cap: Part 1 – Modelling its evolution, sensitivity and associated climate. *Boreas* **42**: 471–490. https://doi.org/10.1111/j.1502-3885.2012.00300.x

Patton H, Hubbard A, Glasser NF *et al*. 2013c. The last Welsh Ice Cap: Part 2 – Dynamics of a topographically controlled icecap. *Boreas* **42**: 491–510. https://doi.org/10.1111/j.1502-3885.2012.00301.x

Peake DS. 1961. Glacial changes in the Alyn river system and their significance in the glaciology of the North Welsh border. *Quarterly Journal of the Geological Society* **117**: 335–363. https://doi.org/10.1144/gsjgs.117.1.0335

Peck VL, Hall IR, Zahn R *et al*. 2006. High resolution evidence for linkages between NW European ice sheet instability and Atlantic Meridional Overturning Circulation. *Earth and Planetary Science Letters* **243**: 476–488. https://doi.org/10.1016/j.epsl.2005.12.023

Peck VL, Hall IR, Zahn R *et al*. 2007. The relationship of Heinrich events and their European precursors over the past 60 ka BP: a multi-proxy ice-rafted debris provenance study in the North East Atlantic. *Quaternary Science Reviews* **26**: 862–875. https://doi.org/10.1016/j.quascirev.2006.12.002

Praeg D, McCarron S, Dove D *et al*. 2015. Ice sheet extension to the Celtic Sea shelf edge at the Last Glacial Maximum. *Quaternary Science Reviews* **111**: 107–112. https://doi.org/10.1016/j.quascirev.2014.12.010

Prescott JR, Hutton JT. 1994. Cosmic ray contributions to dose rates for luminescence and ESR dating: large depths and long-term time variations. *Radiation Measurements* **23**: 497–500. https://doi.org/10.1016/1350-4487(94)90086-8

Rasmussen SO, Bigler M, Blockley SP *et al*. 2014. A stratigraphic framework for abrupt climatic changes during the Last Glacial period based on three synchronized Greenland ice-core records: refining and extending the INTIMATE event stratigraphy. *Quaternary*

© 2021 The Authors *Journal of Quaternary Science* Published by John Wiley & Sons, Ltd.

10991417, 2021, 5, Downloaded from https://onlinelibrary.wiley.com/doi/10.1002/jqs.3313 by Ogs Trieste Istituto Nazionale, Wiley Online Library on [24/11/2023]. See the Terms and Conditions (https://onlinelibrary.wiley.com/terms-and-conditions) on Wiley Online Library for rules of use; OA articles are governed by the applicable Creative Commons License

Science Reviews **106**: 14–28. https://doi.org/10.1016/j.quascirev.2014.09.007

Rasmussen TL, Thomsen E, Moros M. 2016. North Atlantic warming during Dansgaard-Oeschger events synchronous with Antarctic warming and out-of-phase with Greenland climate. *Scientific Reports* **6**: 20535. https://doi.org/10.1038/srep20535. [PubMed: 26847384].

Rhodes EJ. 2011. Optically stimulated luminescence dating of sediments over the past 200,000 years. *Annual Review of Earth and Planetary Sciences* **39**: 461–488. https://doi.org/10.1146/annurev-earth-040610-133425

Roberts DH, Dackombe RV, Thomas GS. 2007. Palaeoice streaming in the central sector of the British—Irish Ice Sheet during the Last Glacial Maximum: evidence from the northern Irish Sea Basin. *Boreas* **36**: 115–129.

Rolfe CJ, Hughes PD, Fenton CR *et al*. 2012. Paired ^{26}Al and ^{10}Be exposure ages from Lundy: new evidence for the extent and timing of Devensian glaciation in the southern British Isles. *Quaternary Science Reviews* **43**: 61–73. https://doi.org/10.1016/j.quascirev.2012.04.003

Scourse JD. 1991. Late Pleistocene stratigraphy and palaeobotany of the Isles of Scilly. *Philosophical Transactions of the Royal Society of London. Series B* **334**: 405–448. https://doi.org/10.1098/rstb.1991.0125

Scourse JD, Austin WEN, Bateman RM *et al*. 1990. Sedimentology and micropalaeontology of glacimarine sediments from the central and southwestern Celtic Sea. *Geological Society, London, Special Publications* **53**: 329–347. https://doi.org/10.1144/GSL.SP.1990.053.01.19

Scourse JD, Austin WEN, Long BT *et al*. 2002. Holocene evolution of seasonal stratification in the Celtic Sea: refined age model, mixing depths and foraminiferal stratigraphy. *Marine Geology* **191**: 119–145. https://doi.org/10.1016/S0025-3227(02)00528-5

Scourse JD, Furze MFA. 2001. A critical review of the glaciomarine model for Irish Sea deglaciation: evidence from southern Britain, the Celtic Shelf and adjacent continental slope. *Journal of Quaternary Science* **16**: 419–434. https://doi.org/10.1002/jqs.629

Scourse JD, Haapaniemi AI, Colmenero-Hidalgo E *et al*. 2009. Growth, dynamics and deglaciation of the last British–Irish ice sheet: the deep-sea ice-rafted detritus record. *Quaternary Science Reviews* **28**: 3066–3084.

Scourse JD, Rhodes EJ. 2006. Battery (Castle Down). In *Isles of Scilly: Field Guide*, Scourse JD (ed). Quaternary Research Association: London; 136–138.

Scourse JD, Saher M, Van Landeghem KJJ *et al*. 2019. Advance and retreat of the marine-terminating Irish Sea Ice Stream into the Celtic Sea during the last glacial: timing and maximum extent. *Marine Geology* **412**: 53–68. https://doi.org/10.1016/j.margeo.2019.03.003

Small D, Clark CD, Chiverrell RC *et al*. 2017. Devising quality assurance procedures for assessment of legacy geochronological data relating to deglaciation of the last British–Irish Ice Sheet. *Earth-Science Reviews* **164**: 232–250. https://doi.org/10.1016/j.earscirev.2016.11.007

Small D, Smedley RK, Chiverrell RC *et al*. 2018. Trough geometry was a greater influence than climate-ocean forcing in regulating retreat of the marine-based Irish-Sea Ice Stream. *GSA Bulletin* **130**: 1981–1999. https://doi.org/10.1130/B31852.1

Smedley RK. 2018. Dust, sand and rocks as windows into the past. *Elements* **14**: 9–14. https://doi.org/10.2138/gselements.14.1.9

Smedley RK, Chiverrell RC, Ballantyne CK *et al*. 2017b. Internal dynamics condition centennial-scale oscillations in marine-based ice-stream retreat. *Geology* **45**: 787–790. https://doi.org/10.1130/G38991.1

Smedley RK, Scourse JD, Small D *et al*. 2017a. New age constraints for the limit of the British–Irish Ice Sheet on the Isles of Scilly. *Journal of Quaternary Science* **32**: 48–62. https://doi.org/10.1002/jqs.2922

Smith BW, Rhodes EJ, Stokes S *et al*. 1990. Optical dating of sediments: initial quartz results from Oxford. *Archaeometry* **32**: 19–31. https://doi.org/10.1111/j.1475-4754.1990.tb01078.x

Telfer, MW, Wilson, P & Lord, TC. (2009) New constraints on the age of the last ice sheet glaciation in NW England using optically stimulated luminescence dating. *Journal of Quaternary Science*, **24**906–915.

Thomas GSP. 1985. The Late Devensian glaciation along the border of northeast Wales. *Geological Journal* **20**: 319–340. https://doi.org/10.1002/gj.3350200403

Thomas GSP. 1989. The Late Devensian glaciation along the western margin of the Cheshire-Shropshire lowland. *Journal of Quaternary Science* **4**: 167–181.

Thomas GSP. 2005. North-East Wales. In *The Glaciations of Wales and Adjacent Areas*, Lewis CA, Richards AE (eds). Logaston Press: Bristol; 41–58.

Thomas GSP, Chiverrell RC. 2007. Structural and depositional evidence for repeated ice-marginal oscillation along the eastern margin of the Late Devensian Irish Sea Ice Stream. *Quaternary Science Reviews* **26**: 2375–2405. https://doi.org/10.1016/j.quascirev.2007.06.025

Thomas GSP, Chiverrell RC. 2011. *Styles of Structural Deformation and syn-Tectonic Sedimentation Around the Margins of the Late Devensian Irish Sea Ice Stream: the Isle Of Man, Llyn Peninsula and County Wexford: Glacitectonics: A Field Guide*. Quaternary Research Association: London; 59–78.

Thomas GSP, Chiverrell RC, Huddart D. 2004. Ice-marginal depositional responses to readvance episodes in the Late Devensian deglaciation of the Isle of Man. *Quaternary Science Reviews* **23**: 85–106. https://doi.org/10.1016/j.quascirev.2003.10.012

Thomas GSP, Summers AJ. 1983. The Quaternary stratigraphy between Blackwater Harbour and Tinnaberna, County Wexford. *Journal of Earth Sciences – Royal Dublin Society* **5**: 121–134.

Thomas GSP, Summers AJ. 1984. Glacio-dynamic structures from the Blackwater Formation, Co. Wexford, Ireland. *Boreas* **13**: 5–12. https://doi.org/10.1111/j.1502-3885.1984.tb00053.x

Tóth Z, McCarron S, Wheeler AJ *et al*. 2020. Geomorphological and seismostratigraphic evidence for multidirectional polyphase glaciation of the northern Celtic Sea. *Journal of Quaternary Science* **35**: 465–478. https://doi.org/10.1002/jqs.3189

Trotter FM, Hollingworth SE, Eastwood T *et al*. 1937. *Gosforth District Geological Survey Memoir, England and Wales, Sheet* **37**.

Van Kreveld S, Sarnthein M, Erlenkeuser H *et al*. 2000. Potential links between surging ice sheets, circulation changes, and the Dansgaard-Oeschger Cycles in the Irminger Sea, 60-18 Kyr. *Paleoceanography* **15**: 425–442. https://doi.org/10.1029/1999PA000464

Van Landeghem KJJ, Chiverrell RC. 2020. Bed erosion during fast ice streaming regulated the retreat dynamics of the Irish Sea Ice Stream. *Quaternary Science Reviews* **245**. https://doi.org/10.1016/j.quascirev.2020.106526

Van Landeghem KJJ, Wheeler AJ, Mitchell NC. 2009. Seafloor evidence for palaeoice streaming and calving of the grounded Irish Sea Ice Stream: implications for the interpretation of its final deglaciation phase. *Boreas* **38**: 111–118.

Waelbroeck C, Lougheed BC, Vazquez Riveiros N *et al*. 2019. Consistently dated Atlantic sediment cores over the last 40 thousand years. *Scientific Data* **6**: 165. https://doi.org/10.1038/s41597-019-0173-8. [PubMed: 31477737].

Wilson P, Rodés Á, Smith A. 2018. Valley glaciers persisted in the Lake District, north-west England, until ~16–15 ka as revealed by terrestrial cosmogenic nuclide (^{10}Be) dating: a response to Heinrich event 1? *Journal of Quaternary Science* **33**: 518–526. https://doi.org/10.1002/jqs.3030

Wintle AG. 1981. Thermoluminescence dating of Late Devensian loesses in southern England. *Nature* **289**: 479–480. https://doi.org/10.1038/289479a0

Wright WB. 1914. *The Quaternary Ice Age*. Macmillan: London.

© 2021 The Authors *Journal of Quaternary Science* Published by John Wiley & Sons, Ltd.

10991417, 2021, 5, Downloaded from https://onlinelibrary.wiley.com/doi/10.1002/jqs.3313 by Ogs Trieste Istituto Nazionale, Wiley Online Library on [24/11/2023]. See the Terms and Conditions (https://onlinelibrary.wiley.com/terms-and-conditions) on Wiley Online Library for rules of use; OA articles are governed by the applicable Creative Commons License